Eur. J. Mineral.
2000, **12**, 543-570

Hydrogen in nominally anhydrous upper-mantle minerals: concentration levels and implications

JANNICK INGRIN* and HENRIK SKOGBY**

*Laboratoire Mécanismes de Transfert en Géologie, U. M. R. 5563, Equipe de Minéralogie, CNRS - Université Paul Sabatier, 39 allées Jules Guesde, 31000 Toulouse, France
e-mail: ingrin@cict.fr
**Department of Mineralogy, Swedish Museum of Natural History, Box 50007, 104 05 Stockholm, Sweden

Abstract: Several of the supposedly anhydrous major minerals of the upper mantle have been shown to regularly contain small amounts of hydrogen. The concentrations measured in the most important minerals obtained from mantle xenoliths are, expressed in ppm H_2O, 100-1300 for clinopyroxene, 60-650 for orthopyroxene, 0-140 for olivine and 1-200 for garnet. Hydrogen is normally structurally incorporated as hydroxyl ions, and in many cases the hydrogen ions seem to act as charge compensators associated with point defects, such as metal vacancies or substitution by mono- or trivalent cations. The determination of the exact amount of hydrogen stored in these nominally anhydrous upper mantle minerals is a key-step toward quantification of the water content of the mantle, as well as understanding of its internal water cycle. For instance, a concentration of 100 ppm H_2O homogeneously distributed within the upper mantle above 410 km depth is approximately equivalent to a 100 m water layer at the Earth's surface. However, the relatively fast kinetics of dehydrogenation with concomitant oxidation of iron within these minerals, implies that hydrogen as well as Fe^{3+} concentrations in equilibrium with mantle conditions might be different from those measured from recovered xenolith samples. High-pressure experimental measurements of hydrogen solubility as a function of p_{H_2O} show a trend similar to the hydrogen contents of natural samples, with hydrogen saturation levels that decrease following the mineral series: diopside > enstatite > olivine > pyrope. Except pyrope, these minerals may incorporate more than 1000 ppm H_2O. Based on recent data of water solubility, stability and partitioning, we suggest that an entire upper mantle saturated in hydrogen is highly unprobable and that the maximum average amount of hydrogen stored in the nominally anhydrous minerals of the upper mantle is around 600 ppm H_2O. Despite the important progress achieved during the last years, our knowledge of the concentration of hydrogen stored as point defects in the mantle above 410 km is still too poorly constrained. The importance of nominally anhydrous minerals for the water budget of the upper mantle is now well established but still awaits complete quantification.

Key-words: hydrogen, water, upper mantle, solubility, kinetics, nominally anhydrous minerals.

1. Introduction

Knowledge of the amount of hydrogen stored in the upper mantle at present – and in the past – is a key problem for understanding the petrological and geochemical evolution of the mantle, as well as for constraining the accretion model of the Earth, the hydrosphere formation and the complete cycle of hydrogen inside the mantle. Hydrogen, structurally bound as point defects in nominally anhydrous minerals (NAM) was first mentioned by Martin & Donnay (1972) as the main site for water storage in the mantle. However, it is only during the past ten years that a larger attention, initiated mainly by the work of G.R. Rossman, has been turned to the study of hydrogen in nominally anhydrous minerals, and especially to upper-mantle minerals. The most im-

0935-1221/2000/0012-0543 $ 7.00

Table 1. References to studies concerning hydrogen incorporation in important nominally anhydrous upper-mantle minerals, in chronological order.

olivine	Martin & Donnay, 1972	clinopyroxene	Martin & Donnay, 1972
	Wilkins & Sabine, 1973		Wilkins & Sabine, 1973
	Beran & Putnis, 1983		Beran, 1976
	Aines & Rossman, 1984a		Ingrin *et al.*, 1989
	Freund & Oberheuser, 1986		Skogby & Rossman, 1989
	Kitamura *et al.*, 1987		Skogby *et al.*, 1990
	Miller *et al.*, 1987		Smyth *et al.*, 1991
	Mackwell & Kohlstedt, 1990		Skogby, 1994
	Bai & Kohlstedt, 1992		Bell *et al.*, 1995
	Bai & Kohlstedt, 1993		Ingrin *et al.*, 1995
	Bell *et al.*, 1994		
	Wright & Catlow, 1994	garnet	Ackermann *et al.*, 1983
	Libowitzky & Beran, 1995		Aines & Rossman, 1984b, c
	Kohlstedt *et al.*, 1996		Rossman *et al.*, 1988
	Kohn, 1996		Lager *et al.*, 1989
	Kurosawa *et al.*, 1997		Rossman *et al.*, 1989
			Geiger *et al.*, 1991
orthopyroxene	Martin & Donnay, 1972		Rossman & Aines, 1991
	Beran & Zemann, 1986		Bell & Rossman, 1992b
	Skogby *et al.*, 1990		Langer *et al.*, 1993
	Mackwell, 1994		Khomenko *et al.*, 1994
	Bell *et al.*, 1995		Bell *et al.*, 1995
	Dobson *et al.*, 1995		Wang *et al.*, 1996
			Lu & Keppler, 1997
			Withers *et al.*, 1998

portant mantle minerals, as deemed from abundance and hydrogen concentration, have shown to be olivine, clinopyroxene, orthopyroxene and garnet, which have been subjected to a large number of studies on the different aspects of hydrogen incorporation. A selection of such articles is given in Table 1. The amount of hydrogen varies strongly, with a range in measured hydrogen concentrations in the mantle-xenolith samples of about 0-200 ppm H_2O for olivine and garnet, and 100-1000 ppm H_2O for pyroxenes, as shown by a data compilation by Bell & Rossman (1992a). These authors conclude, in agreement with others, that the trace-hydrogen-bearing nominally anhydrous minerals probably act as the major repository for H_2O in the Earth's upper mantle (Smyth *et al.*, 1991; Bell & Rossman, 1992a).

Nominally hydrous minerals being present in the upper mantle, such as amphibole, talc, chlorite, phlogopite, lawsonite, dense hydrous magnesium silicates (DHMS; Thompson, 1992), *etc.*, may of course contain considerably higher concentrations of hydrogen. The high-pressure stability fields and dehydration boundaries of these phases are still extensively studied, and the most recent results suggest that they could be important storage sites for water in specific regions of the upper mantle (*e.g.* Schreyer, 1988; Schmidt & Poli, 1994; Pawley & Wood, 1995; Schmidt, 1995; Ulmer & Trommsdorff, 1995; Inoue *et al.*, 1998; Irifune *et al.*, 1998). Most of these phases are stable in the range of P, T conditions prevailing in subduction slabs and can transport water at different depths down to the transition zone (Thompson, 1992). A few of them, like K-amphiboles, could also be stable in hotter regions of the upper mantle, but their abundance is limited by the low concentration of K and Na in the upper mantle (Thompson, 1992). In any case, the hydrous and the nominally anhydrous mineral groups are not exclusive alternatives to water storage in the upper mantle. Both types of phases must be considered in order to describe completely the water cycle in the Earth's interior. Hydrous minerals are probably more important in the water-rich regions of the mantle like subduction zones, while nominally anhydrous minerals may be important in the remainder of the upper mantle,

including the peridotite "conveyor belt" above subduction zones (*cf.* Bell & Rossman, 1992a).

Initially, part of the attention for hydrogen in upper-mantle minerals was linked to the interest in the weakening effect of water on the deformation of mantle minerals, and the possible implication for the rheology of the mantle (Justice & Graham, 1982; Chopra & Paterson, 1984; Aines & Rossman, 1984a; Mackwell *et al.,* 1985; Karato *et al.,* 1986; Drury, 1991; Ingrin *et al.,* 1992; Chen *et al.,* 1998). However, it seems now that the most significant effects caused by hydrogen may concern conductivity (Karato, 1990), stoichiometry, and partial melting of the host mantle minerals (Wyllie, 1979; Kushiro, 1990; Bell & Rossman, 1992a; Gaetani *et al.,* 1993; Raterron *et al.,* 1997).

During the last 10 years, quantitative measurements of the concentration of structurally bound hydrogen in mantle minerals have become reliable, mainly due to the improvement of the accuracy of infrared (IR) spectroscopy calibrations (*e.g.* Bell *et al.,* 1995). A fundamental issue has been to decide how the measurements of hydrogen concentration performed on mantle xenolith samples can be used to determine the true amount of hydrogen stored in the upper mantle. Several authors suggested that large amounts of hydrogen may be lost by xenolith samples, especially olivine, during their ascent (Mackwell & Kohlstedt, 1990; Bai & Kohlstedt, 1992, 1993), while others cast doubts on the importance of dehydrogenation during ascent (Ihinger & Bell, 1991; Bell *et al.,* 1994). Despite two recent review articles (Bell & Rossman, 1992a; Rossman, 1996), the rapidly increasing amount of data collected by European and American laboratories make it difficult to get a clear view of the current knowledge on the subject. In this article, we will successively review: 1) hydrogen concentration data measured in mantle xenolith samples, 2) the recent knowledge on the point defects associated with the structural incorporation of hydrogen, 3) the kinetics of hydrogen exchange reactions, 4) the dependency of hydrogen solubility with pressure, and 5) the relationship between Fe^{3+} and hydrogen contents, for the main anhydrous mantle minerals olivine, clinopyroxene, orthopyroxene and garnet. The aim is to discuss the realistic ranges of hydrogen concentration that can be expected in the upper mantle, in accordance with the more recent mineralogical data, and to direct attention to the main points that still need to be addressed.

2. Hydrogen in mantle xenolith minerals and related point defects

2.1. Analytical methods

Quantitative determination of the sometimes low concentrations of intrinsic hydrogen in nominally anhydrous minerals may be a difficult task. A large number of analytical methods have been applied, and among these, IR spectroscopy has been the most frequently used method. In the IR spectrum the vibrational mode of the OH dipole gives rise to absorption bands, and the position of these bands depends on the strength of the hydrogen bond, bond geometry and neighbours (Libowitzky, 1999). Examples of typical IR spectra of olivine, garnet, orthopyroxene and clinopyroxene in the wavenumber range of the OH stretching bands are shown in Fig. 1. The orientation of the OH dipole may be inferred from the pleochroic behaviour of the absorption bands. The concentration of OH is directly related to the intensities of the bands if the spectra are measured accurately; *e.g.* spectra of anisotropic minerals should be measured in polarised mode (*cf.* Libowitzky & Rossman, 1996). Advantages of the IR technique are very high sensitivity, ability to distinguish hydroxyl ions from adsorbed and intrinsic water molecules, and distinguish OH appearing in inclusions of hydrous phases from OH structurally bound in the parent phase (*e.g.* amphibole lamellae in clinopyroxene, Skogby & Rossman, 1989). The most important disadvantages are the need of single crystals, and the fact that the technique has to be calibrated against an independent hydrogen analysis method. A number of analytical methods have been adopted to calibrate IR spectra, including P_2O_5 cell coulometry (Wilkins & Sabine, 1973), gravimetric techniques (Aines & Rossman, 1984c), nuclear reaction analysis (Rossman *et al.,* 1988), and gas extraction manometry (Bell *et al.,* 1995). Some of the early calibrations have been shown later on to be inaccurate, and the hydrogen content has in many cases been overestimated. To obtain accurate OH concentrations from IR spectra, the calibration needs to be performed for the mineral under study. Since IR spectra in some cases have been shown to substantially change for specimens of the same mineral of different compositions or from different localities, there may even be a need for independent calibrations for the different types of spectra for the same minerals. For a long period such mineral-specific cali-

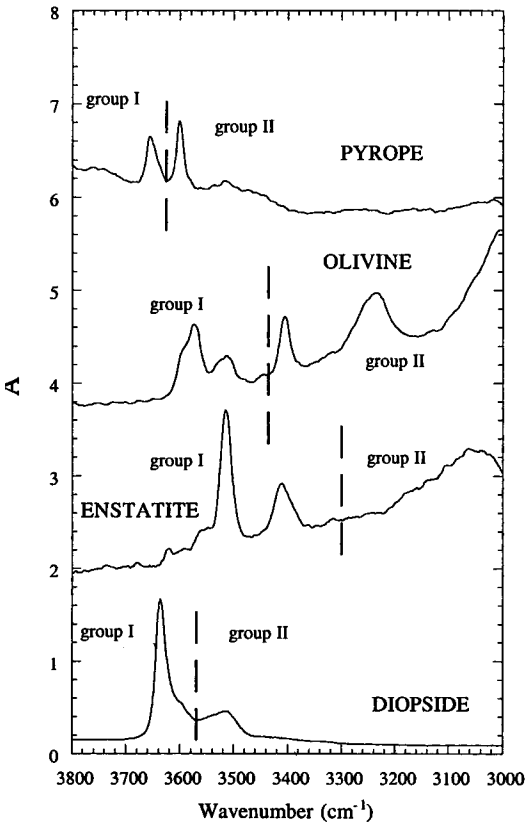

Fig. 1. Example of OH bands present in IR spectra of pyrope, olivine, enstatite, and diopside. Two different types of OH bands are distinguished from pleochroic studies or from the behaviour of the bands with temperature change or with hydrogen incorporation (group I and II). These differences of behaviour suggest that several types of defects are involved in H incorporation in each of these minerals. All spectra were collected on single crystals under the same conditions, resolution 2 cm^{-1}, unpolarized beam and at room temperature. Spectra have not been normalised to common thickness but were vertically offset by A = 2, each. Samples: Dora-Maira pyrope; Zabargad olivine; enstatite from Tanzania; diopside from Russia.

brations were lacking for many mantle minerals, but the recent calibration of Bell *et al.* (1995) has considerably improved the situation for garnet and pyroxenes.

Apart from mineral-specific calibrations of IR spectra a more general calibration method, based on the correlation of the absorption coefficient and the band energy for a number of various hydrous compounds was reported by Paterson (1982) and has often been applied. However, this method cannot be considered as very accurate when applied to different NAM, and concentration data based on this calibration should be treated with some caution. Recently, a new general calibration based on stoichiometric hydrous silicate and oxide minerals was published by Libowitzky & Rossman (1997). The authors emphasize that only spectral areas, and not peak intensities, are correlated with OH concentrations and that proper experimental conditions are a prerequisite to obtain true concentrations (Libowitzky & Rossman, 1996). This new calibration is not profoundly different from the earlier calibration (Paterson, 1982), and is reported with a regression reliability of 10 to 20% (Libowitzky & Rossman, 1997). However, the general applicability of these trends to NAM with low concentrations of H is not yet completely proved and in some cases they differ strongly from mineral-specific calibrations, *e.g.* for pyrope (Libowitzky & Rossman, 1997).

Other methods that have proved useful in determining hydrogen concentrations in NAM are secondary ion mass spectroscopy SIMS (Kurosawa *et al.*, 1992, 1997), and solid state nuclear magnetic resonance (NMR) spectroscopy (Cho & Rossman, 1993; Kohn, 1996).

2.2. Hydrogen contents in xenolith samples

A compilation of the range of hydrogen contents as reported in literature for mantle-derived olivine, clino- and orthopyroxene, and garnet is shown in Fig. 2. The hydrogen contents of the specific minerals, as well as analytical problems and uncertainties, will be discussed below.

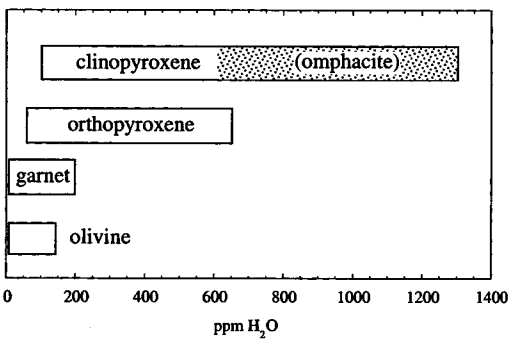

Fig. 2. Range of hydrogen concentration measured in upper-mantle xenoliths. The dashed area for clinopyroxene data corresponds to omphacitic composition.

Olivine

Although olivine has been subjected to a large number of IR studies during recent years, an appropriate calibration by an independent method is still missing. Instead, hydrogen concentrations have usually been calculated from the IR data using the general calibration by Paterson (1982). The uncertainty was therefore substantially higher than for minerals for which accurate mineral-specific calibrations exists, even though the recent calibration of Libowitzky & Rossman (1997) is in fair agreement with the earlier calibration.

Reported hydrogen concentrations for olivine of mantle origin are generally low, often only a few ppm, and range from less than 1 up to 140 ppm H_2O (Miller *et al.*, 1987; Bell & Rossman, 1992a; Rossman, 1996; *cf.* Fig. 2). The higher contents are reported for garnet peridotite and kimberlite megacryst samples, whereas lower contents are reported for spinel lherzolite samples. A recent SIMS study on mantle olivine (Kurosawa *et al.*, 1997) reports concentration levels in the range 10-60 ppm H_2O for a large number of samples. Although this range is compatible with the range obtained by IR spectroscopy, SIMS data from Kurosawa *et al.* (1997) lead generally to higher hydrogen content in spinel lherzolites. For the much studied San Carlos olivine IR band intensities correspond to 0.2-0.6 ppm H_2O (Miller *et al.*, 1987) while SIMS data give considerably higher concentrations of 30-40 ppm H_2O (Kurosawa *et al.*, 1997).

Clinopyroxene

Quantitative determination of hydrogen contents from infrared spectra can now be considered as fairly reliable for diopside and augite since several studies show convergent results (Wilkins & Sabine, 1973; Skogby *et al.*, 1990; Bell *et al.*, 1995). An exception is omphacite, for which no mineral-specific calibration has yet been published. Omphacite spectra are significantly different from augite and diopside spectra, with the main absorption at lower wavenumbers. Since the molar absorption coefficients for OH have been shown to systematically increase toward lower wavenumbers (Paterson, 1982; Skogby & Rossman, 1991; Libowitzky & Rossman, 1997), calculated concentrations for omphacite, based on the diopside calibration, may be somewhat overestimated (Skogby *et al.*, 1990; Smyth *et al.*, 1991). In such cases, the use of a general calibration method (Libowitzky & Rossman, 1997) may be preferred.

Clinopyroxene is the major upper-mantle mineral that has been shown to carry the highest concentrations of hydrogen (*cf.* Bell & Rossman, 1992a; Fig. 2). Concentration data have been reported for diopside, augite and omphacite, and range from 100 to 1300 ppm H_2O (Skogby *et al.*, 1990; Smyth *et al.*, 1991; Bell & Rossman, 1992a; Rossman, 1996). Although the highest concentrations are found in omphacite from mantle eclogites, augite and diopside contain also considerable amounts of hydrogen, corresponding to 400-600 ppm H_2O. The hydrogen content in these phases does not show significant correlation with the type of mantle environment. Based on a correlation of hydrogen content and M2 site vacancies in clinopyroxene from mantle eclogites, Smyth *et al.* (1991) suggested that the hydrogen concentration may reach 2000 ppm H_2O at depth.

Orthopyroxene

There are few studies of hydrogen contents in mantle orthopyroxenes, and the calibration of the IR spectroscopic data has remained uncertain until the mineral-specific calibration of Bell *et al.* (1995). Skogby *et al.* (1990) report concentrations in the range 60 to 250 ppm H_2O, but these values should be reduced by a factor of 0.4 according to the new calibration. Bell & Rossman (1992a) and Rossman (1996) found that most mantle orthopyroxenes fall in the range 60-650 ppm H_2O, with a few exceptions at lower concentrations represented by basalt megacrysts (Fig. 2). Orthopyroxene in garnet-peridotite xenoliths show the highest concentrations, whereas spinel peridotite show lower concentrations.

Garnet

Mantle pyrope-rich garnets have been subjected to a large number of studies involving OH analyses (*e.g.* Aines & Rossman, 1984b, c; Rossman *et al.*, 1989; Bell & Rossman, 1992a, b; Langer *et al.*, 1993). Reported concentrations range from less than 1 up to 200 ppm H_2O, with most samples containing less than 60 ppm (Bell & Rossman, 1992a; Fig. 2). Significantly higher concentrations have been reported (Aines & Rossman, 1984b; Langer *et al.*, 1993), but new calibrations have

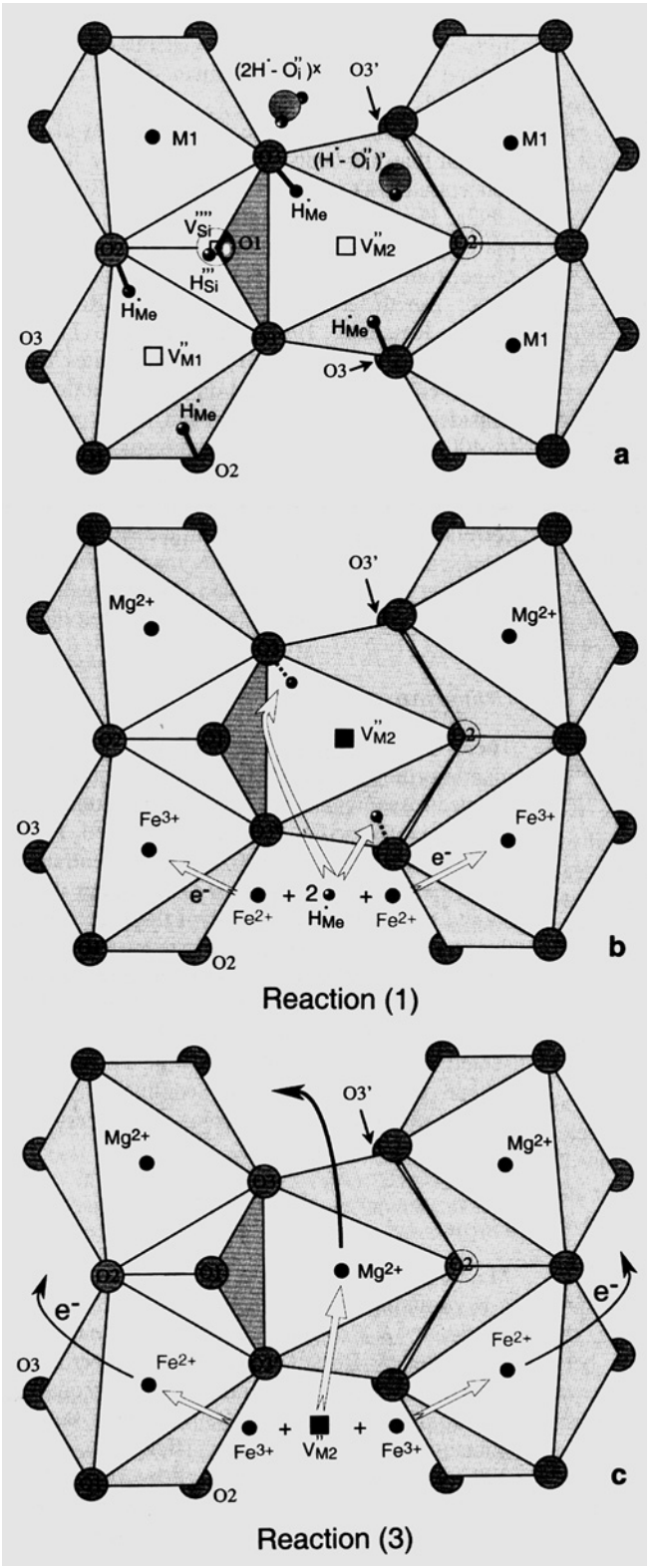

Fig. 3. Schematic diagram of expected hydrogen defects in olivine and upper-mantle nominally anhydrous minerals (NAM) in general, and related reactions of formation of these defects.

a. Hydrogen defects in the olivine structure as suggested by several authors (Freund & Oberheuser, 1986; Bai & Kohlstedt, 1993; Libowitzky & Beran, 1995). The crystallographic structure is projected on the (100) plane and only four M1 octahedral sites, one M2 site and one tetrahedral Si site are shown. Hydrogen defects associated with M1, M2 and Si vacancies (squares): $(2\ H^{\bullet}_{Me} - V''_{M1})^{x}$, $(2\ H^{\bullet}_{Me} - V''_{M2})^{x}$ and $(H^{\bullet}_{Si} - V''''_{Si})'''$ are shown with the orientation of OH bonds in accordance with the pleochroism observed in the infrared spectra. For the possible hydrogen defects associated with oxygen interstitials $(H^{\bullet} - O''_{i})'$ and $(2\ H^{\bullet} - O''_{i})^{x}$ no locations or dipole orientations have been proposed by the authors (Bai & Kohlstedt, 1993), we have projected them close to the much larger empty sites of the structure.

b. Schematic view of the reaction of hydrogenation (1) in the olivine structure: $2\ Fe^{3+} + 2\ O^{2-} + H_2 = 2\ Fe^{2+} + 2\ OH^{-}$, leading to the formation of a $2\ H^{\bullet}_{Me}$ defect attached to a pre-existing M2 vacancy V''_{M2}.

c. Schematic view of a reaction of formation of a "non-hydrogen point defect" (3) in the olivine structure: $2\ Fe^{2+} + Mg_{M2}^{x} + 1/2\ O_2 = 2\ Fe^{3+} + V_{M2}'' + MgO$, leading to the formation of a M2 vacancy V''_{M2}. The kinetics of reaction (3) is much slower than the reaction of hydrogenation (1).

shown these values to be overestimations (*e.g.* Bell *et al.*, 1995).

Different types of systematic variations of the hydrogen concentration in mantle garnets have been reported. From a study based on 166 mantle garnets, Bell & Rossman (1992b) demonstrated that the hydrogen concentration varies according to the host-rock paragenesis, with the lowest values obtained for on-craton eclogites and the highest values obtained for Cr-poor megacrysts. An inverse correlation between hydrogen content and molar fraction X_{Fe} = Mg/(Mg+Fe) for Cr-poor garnet megacryst nodules was interpreted as reflecting the increasing water content of a differentiating parental magma. Moreover, samples from the Colorado plateau, which represent a fluid-rich mantle, have been shown to contain approximately two times more hydrogen than samples from southern Africa (Aines & Rossman, 1984b; Bell & Rossman, 1992a, b).

2.3. Location of OH and associated defects

Although the amount of hydrogen in most nominally anhydrous mantle silicates is relatively easily accessible, it is more difficult to determine the modes of incorporation and the specific crystallographic positions. Since the amount of hydrogen in these minerals is low (<0.13 wt.% H_2O), direct methods such as X-ray and neutron diffraction have rarely been used. The current knowledge is in most cases based on results from indirect methods such as the pleochroic behaviour of IR absorption bands, thermodynamic defect chemistry, correlation with minor elements, and energetic calculations. Since the incorporation mechanisms for hydrogen in both mantle and crustal samples are thought to be similar, results from studies on samples from both types of environments will be considered below.

Olivine

Most point-defect models have involved Si and Mg vacancies (*e.g.* Mackwell & Kohlstedt, 1990), and some also oxygen interstitials (Fig. 3a). Based on experimental results showing that the hydrogen solubility depends on hydrogen fugacity to the first power and oxygen fugacity to the one-half power, Bai & Kohlstedt (1992) proposed an incorporation model with hydrogen associated with oxygen interstitials and Mg vacancies. Due to the appearance of two groups of OH bands (labelled as group I and group II; Fig. 1) and the dependence of hydrogen solubility on both oxygen fugacity and orthopyroxene activity, these authors suggest that hydrogen atoms associated with oxygen interstitials occur together with two distinct lattice defects, one being linked with divalent oxygen interstitials (water molecules) and the other being linked with monovalent oxygen interstitials (hydroxyl ions; Fig. 3a; Bai & Kohlstedt, 1993).

The association of OH with Si and Mg vacancies is compatible with results from studies of the pleochroic behaviour of IR absorption bands (*e.g.* Beran & Putnis, 1983). In a study performed on a natural forsterite sample showing only group-I OH bands in its IR spectrum, Libowitzky & Beran (1995) proposed that oxygen in the O1 position is partially replaced by OH dipoles pointing towards an assumed vacant Si-site. They also noticed that OH at the O2 position and directed towards an assumed vacant M1 octahedron conform to the observed polarisation scheme (Fig. 3a).

However, results based on energetic calculations are not in full agreement with these defect models. Using atomistic computer simulation techniques, Wright & Catlow (1994) investigated the structures and energies of four different OH defects in olivine. Incorporation of hydrogen at an oxygen position accompanied by reduction of ferric iron was found to be the energetically most favourable mechanism. Incorporation of interstitial water molecules associated with Fe^{3+} reduction and Mg vacancies was found to be energetically possible under strongly reducing conditions, whereas incorporation mechanisms involving Si and Mg vacancies alone, and also the hydrogarnet substitution, ($V_{Si}[OH]_4$), were found to be energetically unfavourable. Nevertheless, Mg and Si vacancies have been shown to be present in significant amounts in natural olivine (Nakamura & Schmalzried, 1983), and reduction of ferric iron cannot solely explain the hydrogen concentrations experimentally incorporated at elevated pressures (Bai & Kohlstedt, 1993; Kohlstedt *et al.*, 1996).

Hydrogen incorporation in olivine seems normally not to be directly correlated with the concentration of other elements, although Kurosawa *et al.* (1997) observed a correlation between the sum of the monovalent cations (H+Li+Na) and trivalent cations in olivine from garnet peridotites. In one case, however, a coupled substitution in-

volving hydrogen and other low-concentration elements has been demonstrated in olivine. In a sample of non-mantle origin Sykes *et al.* (1994) report evidence for association of unusually high amounts of hydrogen with boron. They could show by TEM studies that the main incorporation mechanism for the OH determined from IR spectroscopy was *via* the coupled substitution $B(F,OH)Si_{-1}O_{-1}$, and to a minor extent also related to humite-type planar defects.

Clinopyroxene

In the clinopyroxene structure, the O2 oxygen position has been pointed out as a favourable site for the OH ion due to its underbonded character, according to its Pauling bond strength (Smyth, 1988). The excess charge created by the $OH^- \Rightarrow O^{2-}$ substitution may be balanced by either cation vacancies or charge-deficient substitutions (*e.g.* trivalent ions for Si).

Polarised IR spectroscopic studies of diopside have revealed OH absorption bands with two types of pleochroic behaviour, the first (group I) corresponding roughly to bands around 3640 cm^{-1}, and the second (group II) to bands at 3535, 3460 and 3355 cm^{-1} (Fig. 1). These two types of bands suggest that at least two types of hydrogen locations exist simultaneously in the diopside structure (Beran, 1976; Ingrin *et al.*, 1989; Skogby *et al.*, 1990). The OH bands in polarised spectra of augite are similar to diopside spectra, with the exception that the band at 3355 cm^{-1} is missing (Skogby *et al.*, 1990).

Smyth *et al.* (1991) found a correlation of the intensity of a strong OH absorption band at 3470 cm^{-1}, characteristic of jadeite-rich omphacite spectra, and vacancies on the M2 site. They suggested that the OH dipole occupies the O2 oxygen position, and is directed towards a vacant M2 site. This interpretation is supported by experimental studies that have demonstrated that some clinopyroxenes contain octahedral vacancies at the pressure and temperature conditions where eclogite is stable (Gasparik, 1986). The same dipole orientation is reported from studies based on the pleochroic scheme of the higher frequency OH bands (group I) in diopside spectra (Beran, 1976).

Sample chemistry has been demonstrated to correlate to some extent with the intensity of various absorption bands in a few cases. For instance, chromium has been noted to be associated with a specific band in diopside spectra (Ingrin *et al.*, 1989), and other trivalent cations have been shown to be weakly correlated with the intensity of the group II bands (Skogby *et al.*, 1990). Si-deficient ferrian diopsides have been shown to accommodate unusually large amounts of OH under reducing experimental conditions (Skogby & Rossman, 1989).

Orthopyroxene

Reports considering the OH location in orthopyroxene are scarce. IR spectra of orthopyroxenes are different from clinopyroxene spectra, and contain several OH absorption bands. The orthopyroxene OH bands may be also divided into two groups, one consisting of relatively sharp high-energy bands at 3650-3400 cm^{-1} (group I) and the other consisting of broad low-energy bands at 3400-3000 cm^{-1} (group II; Fig. 1). An incorporation model based on the pleochroism of bands from group I of enstatite was presented by Beran & Zemann (1986). They suggested that OH occupies the O2B oxygen position, with a dipole alignment approximately in the [001] direction. The pleochroic scheme and OH orientation have been confirmed for a number of samples by Skogby *et al.* (1990). Also for orthopyroxene, more than one type of defect seems to be involved in the incorporation of hydrogen, as suggested by the occurrence of a broad OH band around 3050 cm^{-1} with only weak pleochroic behaviour (Beran & Zemann, 1986; Skogby *et al.*, 1990; Rauch & Keppler, 1996; Fig. 1).

Garnet

The incorporation mode of OH in garnets has been discussed in numerous studies (*e.g.* Aines & Rossman, 1984b, c; Ackermann *et al.*, 1983; Lager *et al.*, 1989; Rossman & Aines, 1991; Geiger *et al.*, 1991; Cho & Rossman, 1993; Langer *et al.*, 1993; Khomenko *et al.*, 1994; Wright *et al.*, 1994). The hydrogarnet substitution, $(O_4H_4) \Rightarrow SiO_4$, represents the best characterised type of OH incorporation in garnets, and has been verified by both X-ray and neutron diffraction studies (*e.g.* Lager *et al.*, 1989). In addition, atomistic simulation calculations (Wright *et al.*, 1994)

conducted on the grossular structure have shown that the hydrogarnet defect is energetically favourable, and that such defects should be common in garnets. However, the hydrogarnet substitution seems not to be the only incorporation mechanism, even in grossular. At low hydrogen concentrations, IR spectra of grossular are much more complex than at high hydrogen concentrations, and NMR studies of such samples have shown that the OH ions occur in pairs of two rather than in clusters of four (Cho & Rossman, 1993).

The presence of the hydrogarnet substitution with up to several wt.% H_2O has been well established only for garnets of the grossular-andradite series, and it is unclear whether this incorporation mechanism is common in the pyrope-rich garnets of mantle origin. Lager *et al.* (1989) conclude that mantle garnets may contain only very limited amounts of the hydrogarnet component, as indicated from distance-least-squares modelling. Geiger *et al.* (1991) interpret a single-band IR spectrum obtained on synthetic pyrope grown from oxides as being due to the hydrogarnet component. On the other hand, pyrope grown from gels exhibits four bands that resemble spectra of natural near end-member pyrope (Rossman *et al.*, 1989), indicating that OH are present in several different local environments. However, clear correlations of OH bands and minor elements in garnets have not been demonstrated, and Bell & Rossman (1992b) conclude from an extensive study that none of the analysed chemical components seem to facilitate OH incorporation. A defect related to the hydrogarnet substitution, *i.e.* $[(OH_3)O]^{5-}$ groups substituting for SiO_4 groups, has been suggested to occur in synthetic titanium-substituted pyrope (Khomenko *et al.*, 1994).

Additional evidence for multiple incorporation mechanisms are provided from the behaviour of absorption bands after annealing experiments at high pressures and temperatures. Experiments of water incorporation in Dora-Maira pyrope by Lu & Keppler (1997) show that the increase of the OH content in this garnet is related to an intensity increase of the IR bands around 3650 cm^{-1}, while the intensities of the bands around 3600 cm^{-1} decrease (Fig. 1). This behaviour suggests, by comparison with the other minerals considered above, that more than one type of defect seems to be involved in the hydrogen incorporation in pyrope garnet as no particular single OH defect has yet been proposed to explain such variations in band intensities.

3. Mechanisms and kinetics of hydrogen exchange reactions

As mentioned above, the defects associated with hydrogen incorporation in anhydrous minerals may be quite numerous and complex. The hydrogen incorporation mechanisms can be regarded as the combination of a "non-hydrogen point defect" (a cation vacancy, an anion interstitial or a substitution by a cation with a lower valency) associated with one (or several) interstitial hydrogen ions which act(s) as a local charge compensator (Fig. 3a). The exchange of hydrogen with the environment may proceed by two different types of mechanisms: 1) by moving hydrogen interstitials without moving the associated "non-hydrogen point defect" and locally adjusting the charge balance by oxidation of a neighbouring cation, *e.g.* by changing Fe^{2+} into Fe^{3+} (or another multivalent cation; Fig. 3b), 2) by moving also the associated "non-hydrogen point defect", thus suppressing the need for a local charge balance by hydrogen ions (Fig. 3c).

The first type of mechanism requires diffusion of hydrogen ions (protons) coupled with a counter flux of electron holes, related to the valence change of multivalent cations (Fe, Mn; Fig. 3b). The second type of mechanism requires in addition the diffusion of the related point defects (cation vacancies, oxygen interstitials, *etc.*; Fig. 3c). Reactions of the first type are expected to have a considerably faster kinetics than the second type of mechanism (several orders of magnitude). The first type will be active at low temperatures (< 1000 °C) on the time-scale of laboratory experiments while the second type of mechanism will be effective only at higher temperatures and/or for longer durations. The kinetics of oxidation-dehydrogenation and reduction-hydrogenation reactions controlling the exchange of hydrogen between anhydrous minerals and their environment (mechanism 1) begin to be quite well documented. However, the reactions of defect formation that control the maximum of hydrogen solubility in the mineral (mechanism 2) are different for each type of associated "non-hydrogen point defect" and are still poorly constrained.

3.1. Hydrogenation-dehydrogenation reactions

The reaction which is generally assumed to control the hydrogenation-dehydrogenation of an-

Table 2. Reported kinetic data for the dehydrogenation-hydrogenation reaction for olivine, garnet and pyroxene.

Mineral X_{Fe} = Fe/(Fe+Mg)	Orien-tation	T range (°C)	Environment (GPa)	E ± (3σ) (kJ/mole)	D_0 (m^2/s)	Experiment	Refer-ences#
olivine	// **a**	800	P = 0.3 GPa	130 ± 30	$(6 \pm 3)\cdot10^{-5}$	H uptake	
San Carlos	// **c**	-	$-19.4 < \log f_{O_2} < -11.1$	130 ± 30	$(5 \pm 4)\cdot10^{-6}$	-	[1]
X_{Fe} = 9%	// **b**	1000	$f_{H_2} \approx 160$ MPa	?	$< 3\cdot10^{-12}$	IR profiles	
olivine	// **a**	800	P = 0.3 GPa	145 ± 30	$1.4\cdot10^{-4}$	H uptake	
San Carlos	// **c**	-	Fe/FeO and opx buffer	110 ± 50	$1.4\cdot10^{-7}$	-	[2]
X_{Fe} = 9%	// **b**	1000		180 ± 50	$1.5\cdot10^{-4}$	IR profiles	
pyrope		700				H	
		-	in air and N_2 flow	253 ± 20	2 - 5	extraction,	[3]
X_{Fe} = 16%		950				IR profiles	
pink pyrope						H	
Dora Maira		800	in air		$< 2\cdot10^{-14}$	extraction,	[4]
X_{Fe} = 2.5%						IR integral	
diopside		700				H	
X_{Fe} = 3.6%	//	-	in air	126 ± 24	$2\cdot10^{-7}$	extraction,	[5], [6]
	a*, b, c	1000	and			H uptake,	
			f_{H_2} = 0.1, 0.01 MPa			IR integral	
diopside		600				H-D	
X_{Fe} = 3.6%	**//a*, c**	-	$f_{H_2} = f_{D_2}$ = 0.01 MPa	149 ± 16	$4\cdot10^{-4}$	exchange	[6]
		850	$-25 < \log f_{O_2} < -16$			IR integral	
diopside		700				H-D	
X_{Fe} = 3.6%	**//b**	-	$f_{H_2} = f_{D_2}$ = 0.01 MPa	143 ± 33	$1\cdot10^{-5}$	exchange	[6]
		900	$-25 < \log f_{O_2} < -16$			IR integral	

[1], Mackwell & Kohlstedt (1990); [2], Kohlstedt & Mackwell (1998); [3], Wang *et al.* (1996); [4], Ingrin & Hercule (1994); [5], Ingrin *et al.* (1995); [6], Hercule & Ingrin (1999).

hydrous iron-containing minerals involves reduction-oxidation of iron, following the reaction (Fig. 3b):

$$Fe^{3+} + O^{2-} + 1/2\ H_2 = Fe^{2+} + OH^- \quad (1)$$

alternatively written:

$$2\ Fe^{3+} + 2\ O^{2-} + H_2O = 2\ Fe^{2+} + 2\ OH^- + 1/2\ O_2,$$

or with the Kröger-Vink notation:

$$Fe_{Me}^{\bullet} + O_O^{x} + 1/2\ H_2 = Fe_{Me}^{x} + (OH)_O^{\bullet}$$

with "•" for one extra positive charge and "x" for a normal charge in regard to the occupied site. This reaction was first proposed by Barnes (1930) for the dehydrogenation of amphiboles. The correlation of hydrogen loss with Fe^{3+} increase during heating has been confirmed by IR and Mössbauer spectroscopic studies (Patterson & O'Connor, 1966; Ernst & Wai, 1970). Since these early works, numerous studies of dehydrogenation have been performed on amphiboles with different compositions, which have confirmed the impor-

tance of this reaction (see for instance Hawthorne, 1981; Clowe *et al.*, 1988; Phillips *et al.*, 1989; Dyar *et al.*, 1992, 1993). These studies on hydrous minerals have been used largely as guides for the study of low-temperature hydrogen exchange in anhydrous mantle minerals.

Recent results of kinetic studies suggest that for iron-rich minerals (above an X_{Fe} = Fe/(Fe+Mg) ratio of about 0.08, close to the average of the upper-mantle composition) the kinetics of reaction (1) is rate-limited by the mobility of the hydrogen atoms whereas, for lower iron contents, it is slower and controlled by the mobility of electron holes (Hercule & Ingrin, 1999; Carpenter *et al.*, 2000). In general, the kinetics of exchange is anisotropic (olivine and pyroxenes) if it is controlled by hydrogen mobility, but isotropic if it is limited by the electron-hole mobility. As will be discussed below the kinetics of the hydrogenation-dehydrogenation reaction for the different upper mantle NAM in the temperature range 700-1000 °C are very close to each other, within one order of magnitude (Fig. 4). With an average diffusion coefficient around 10^{-10} m²/s at 1000 °C, hydrogen exchange by reaction (1) is very fast, and equilibration should be attained within less than tens of hours for the majority of crystals at this temperature.

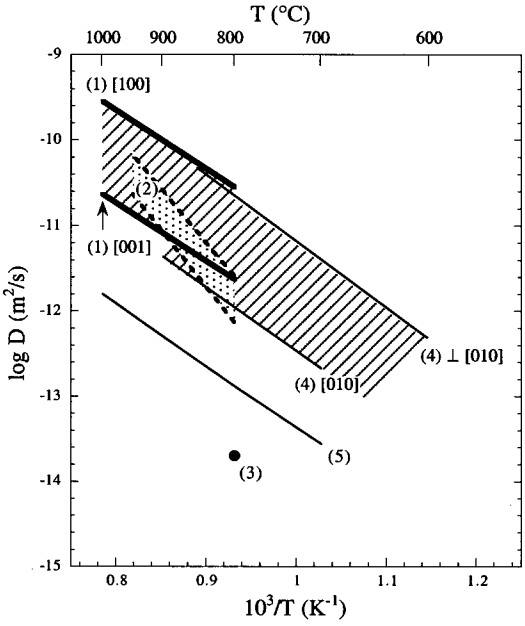

Fig. 4. Arrhenius plot summarising the kinetics of dehydrogenation-hydrogenation reactions and H-D exchange in olivine (bold lines), pyrope (dashed lines and dot), diopside (thin lines). All the shaded area represents the expected range of H exchange in upper mantle NAM (controlled by H diffusion). The crystallographic directions of diffusion are indicated for minerals with anisotropic behaviour. (1) H incorporation in San Carlos olivine, Mackwell & Kohlstedt (1990); (2) H extraction in iron-rich pyrope, Wang *et al.* (1996); (3) H extraction in iron-poor Dora-Maira pyrope, Ingrin & Hercule (1994); (4) H-D exchange in diopside, Hercule & Ingrin (1999); (5) H extraction in iron-poor diopside, Ingrin *et al.* (1995).

Olivine

The first qualitative kinetic study of hydrogenation in olivine (San Carlos) was performed by Mackwell *et al.* (1985) and showed that the rate of exchange is very fast at 1100 °C (saturation after few hours for a 3 mm thick sample). Later on, the same material was subjected to a quantitative kinetic study in the temperature range 800-1000 °C (Mackwell & Kohlstedt, 1990). These results showed that the rate of hydrogenation at 0.3 GPa in San Carlos olivine is strongly anisotropic with diffusion coefficients along crystallographic direction $D_a \approx 10D_c \geq 100D_b$ and an activation energy for both *a* and *c* directions equal to 130 ± 30 kJ/mol (Table 2; Fig. 4). The diffusion rate is not affected by the hydrogen concentration in the studied range of concentrations and seems qualitatively not affected by oxygen fugacity. The authors finally suggest that the kinetics of hydrogen incorporation in olivine is controlled by the diffusion of hydrogen through reaction (1), the mobile species being protons charge-coupled to a counter flux of electron holes.

Clinopyroxene

Low-temperature extraction and incorporation of hydrogen in clinopyroxenes was reported by Ingrin *et al.* (1989) and Skogby & Rossman (1989). Both papers suggest that hydrogen exchange is controlled by the oxidation-dehydrogenation reaction (1), which is supported by results from optical spectroscopy showing that hydrogen uptake (at 700 °C under 1 atm H_2) is correlated with an increase of Fe^{2+}. More recently, Skogby (1994) has shown from hydrogen incorporation experiments on synthetic crystals studied by Mössbauer spectroscopy, that octahedrally coordinated Fe^{3+} is reduced to Fe^{2+} by an amount somewhat higher than the amount of incorporated hydrogen. The

kinetics of the hydrogenation-dehydrogenation reaction has been particularly well documented for diopside (Ingrin *et al.*, 1995; Hercule, 1996; Carpenter, 1996; Hercule & Ingrin, 1999; Carpenter *et al.*, 2000; Skogby, unpublished data).

Experiments performed in air and at 0.1 and 1 atm p_{H_2} on diopside single crystals with X_{Fe} = Fe/(Fe + Mg) = 0.036 followed by IR spectroscopy in the range 700-1000 °C have shown that the kinetics of the hydrogenation-dehydrogenation reaction is isotropic, and one to two orders of magnitude slower than hydrogenation of olivine (Ingrin *et al.*, 1995; Hercule & Ingrin, 1999; Fig. 4). The activation energy of diffusion is close to the activation energy found for olivine (126 ± 24 kJ/mol; Table 2). However, hydrogen-deuterium exchange performed on the same samples in the same range of temperature at 0.1 atm p_{H_2} and p_{D_2}, leads to faster diffusion coefficients, that are much closer to the diffusion coefficients for olivine. The H-D exchange is found to be anisotropic with $D_a \approx D_c \approx 10D_b$ and an activation energy in the same range as for hydrogenation-dehydrogenation of olivine and diopside (around 145 kJ/mole; Hercùle & Ingrin, 1999; Table 2, Fig. 4). These authors conclude that reaction (1) is not rate-limited by the mobility of hydrogen in iron-poor diopside, but more probably by the mobility of electron holes.

As suggested by early studies (Bai *et al.*, 1994; Skogby, 1994) and quantified by recent dehydrogenation experiments performed in air on diopside single-crystals with various iron content (X_{Fe}: 0.064, Carpenter, 1996; Carpenter *et al.*, 2000; 0.05, 0.126, Hercule, 1996; 0.05-0.29, Skogby, hydrogenation, unpublished data), the kinetics of reaction (1) increase with the iron content, up to a maximum rate which corresponds to the mobility of hydrogen. This rate limit is reached at X_{Fe} = 0.06-0.08 (Hercule, 1996).

In none of the studies mentioned above has a dependence of the hydrogen exchange kinetics on the hydrogen and oxygen partial pressures been reported.

Orthopyroxene

Almost all the dehydrogenation-hydrogenation experiments performed on orthopyroxenes are qualitative (Beran & Zemann, 1986; Skogby & Rossman, 1989; Bell *et al.*, 1995). A rough calculation from the sparse data suggests that the kinetics of dehydrogenation is in the range of the kinetics observed for diopside and olivine. Skogby & Rossman (1989) assume, by analogy with clinopyroxene, that hydrogen exchange in enstatite is governed by reaction (1). However, no clear proof has yet been published. Preliminary quantitative kinetic data have been presented by Mackwell (1994); however, the results were difficult to interpret due to the different behaviour observed for the individual OH absorption bands.

Garnet

Although a large number of IR analyses of hydrogen defects in garnets have been performed (especially interesting for the present review are the pyrope-rich mantle garnets), only very few kinetic experiments have been reported. Despite the fact that low-temperature dehydrogenation of garnet on the time scale of laboratory experiments has been demonstrated, it is generally assumed that hydrogen in pyrope is less easily removed than hydrogen in other anhydrous minerals (Geiger *et al.*, 1991; Bell *et al.*, 1995). This view is confirmed by recent dehydrogenation experiments performed on iron-rich pyrope single-crystals (around 16 % almandine component) by Wang *et al.* (1996) who obtained kinetic rates around one order of magnitude slower than those obtained for olivine and diopside (Fig. 4). The authors found that the kinetics of dehydrogenation in pyrope depends on the hydrogen concentration of the pyrope crystal. Their study also shows that the activation energy of the diffusion process involved in the dehydrogenation reaction in these garnets is much higher than that measured for olivine or diopside (253 ± 20 kJ/mol; Table 2). However, for more iron-poor garnet (sample from Dora-Maira Massif with about 2.5 % of almandine component) Ingrin & Hercule (1994) found, at 800 °C, that the kinetics is at least thirty times slower than that obtained by Wang *et al.* (1996) (Fig. 2; Table 2). This suggests that the kinetics of reaction (1) may be positively correlated with the iron content also in garnet.

General comments

The main points which should be emphasised from the results of the kinetic studies of reaction (1) in mantle NAM are:

1) There is only a small variation in the kinetics of hydrogen exchange in iron-rich olivine, pyroxene and garnet. In the temperature

range 800-1000 °C the kinetics are within one order of magnitude (Fig. 4).

2) The dependence of the kinetics on iron content, as demonstrated for diopside and indicated for garnet, is highly probable for all these minerals if they have a low concentration of iron (X_{Fe} less than 0.08). The high concentration of iron in upper mantle NAM (X_{Fe} generally above 0.08) suggests that the kinetics of H exchange following reaction (1) is probably rate-limited by the diffusion of hydrogen in these minerals (shaded area in Fig. 4).

3) The low activation energies of the kinetics of the exchange reactions (130-140 kJ/mol) observed for olivine and pyroxene compared to the higher activation energy (250 kJ/mol) observed for garnet suggest that the types of defects involved in the storage of hydrogen in garnets are different from those of olivine and pyroxenes. The activation energies found for garnet are closer to the activation energies found for H exchange in quartz and feldspars (160-200 kJ/mol, Kats *et al.*, 1962; Kronenberg *et al.*, 1986; Behrens, 1994; Kronenberg *et al.*, 1996).

3.2. Reactions involved in the formation of hydrogen-associated point defects

The concentration of "non-hydrogen point defects" associated with hydrogen interstitials determines the maximum amount of hydrogen that can be incorporated at a given hydrogen fugacity (f_{H_2}) following reaction (1). It is possible to modify the concentration of these defects by reequilibrating the mineral with a different thermodynamic environment during pre-annealing high-temperature experiments. Such experiments were first reported on olivine crystals. Due to the slower kinetics of defect formation in pyroxenes, it is only recently that such experiments have been performed with success in the latter minerals and only preliminary results are reported here.

Olivine

Bai & Kohlstedt (1992, 1993) have shown that the amount of hydrogen which can be incorporated at a given f_{H_2} in olivine (San Carlos) pre-annealed at 1300 °C, is a function of the oxygen fugacitiy (f_{O_2}) and the orthopyroxene activity (a_{opx}) sustained by the sample during the pre-annealing. To explain the observed relationship between f_{O_2} and hydrogen solubility these authors have proposed that hydrogen defects are related to oxygen interstitials (O_i") or/and metal vacancies (V_{Me}", Me cations, Fe, Mg, Ni, Mn, Ca, *etc.*, may occupy either the M1 or M2 octahedral site). The related hydrogen point defects are respectively OH and H_2O interstitials ($(H^{\bullet}- O_i")'$, $(2H^{\bullet} - O_i")^x$) or H atoms located at empty Me sites (H_{Me}' or $(2H)_{Me}^x$, *cf.* Fig. 3a). Bai & Kohlstedt proposed that the concentrations of these defects are controlled by the following reactions, among others.

Creation of a doubly charged oxygen interstitial,

$$2\ Fe^{2+} + 1/2\ O_2 = 2\ Fe^{3+} + O_i", \qquad (2)$$

where " indicates two extra negative charges, with the two possible associated hydrogen defects following equation (1):

$$Fe_{Me}^{\bullet} + O_i" + 1/2H_2 = Fe_{Me}^x + (H^{\bullet} - O_i")',$$

and

$$Fe_{Me}^{\bullet} + (H^{\bullet} - O_i")' + 1/2\ H_2 = Fe_{Me}^x + (2H^{\bullet} - O_i")^x;$$

or/and (Fig. 3b):

creation of a doubly charged cation vacancy,

$$2\ Fe_{Me}^x + Me_{Me}^x + 1/2\ O_2 = 2\ Fe_{Me}^{\bullet} + V_{Me}" + MeO, \qquad (3)$$

with the two possible associated hydrogen defects following equation (1):

$$Fe_{Me}^{\bullet} + V_{Me}" + 1/2\ H_2 = Fe_{Me}^x + H_{Me}',$$

and

$$Fe_{Me}^{\bullet} + H_{Me}' + 1/2\ H_2 = Fe_{Me}^x + (2H)_{Me}^x.$$

The relaxation times of creep experiments (Mackwell *et al.*, 1988), but also the Fe-Mg interdiffusion measurements (Nakamura & Schmalzried, 1984), and the reequilibration time of fluid inclusions in olivine (Pasteris & Wanamaker, 1988), lead these authors to suggest that the modification of point-defect concentration following the change in the thermodynamic environment surrounding olivine crystals is rate-limited by the mobility of metal vacancies V_{Me}. The activation energy for diffusion of these vacancies is close to 190 kJ/mole, with a D_0 in the range of $2 \cdot 10^{-4}$ m^2/s (Fig. 5; Nakamura & Schmalzried, 1984; Mackwell *et al.*, 1988). It is not yet clear if the new thermodynamic state reached by the interior of the crystal through the migration of metal vacancies V_{Me} is really a true equilibrium or only a

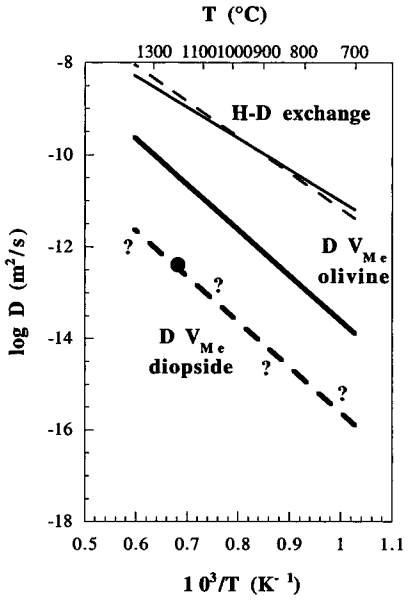

Fig. 5. The high-temperature reequilibration of associated "non-hydrogen point defects" is probably controlled by the mobility of metal vacancies V_{Me}. $D_{V_{Me}}$ in olivine is deduced from a compilation of data of Nakamura & Schmalzried (1984), Mackwell *et al.* (1988) and Kohlstedt & Mackwell (1998), the range of dispersion of data is about 0.5 in logarithmic units along the line labelled "$D_{V_{Me}}$ olivine". The mobility of V_{Me} in diopside at 1200 °C (point) is deduced from Guilhaumou *et al.* (1999). The dashed line "$D_{V_{Me}}$ diopside" is hypothetical (question marks), assuming the same slope than the olivine curve. For comparison also the kinetic relations for hydrogen diffusion in olivine (narrow lines, direction [100]) and diopside (directions [100] and [001]) are plotted.

partial equilibrium of the octahedral sublattice (Poumellec & Jaoul, 1984). As shown by Bai & Kohlstedt (1993), the change of concentration of the "non-hydrogen point defects" involved in the storage of hydrogen in olivine follows the same type of kinetics. Such relatively fast kinetics are more difficult to interpret in terms of the mobility of oxygen interstitials compared to metal vacancies because oxygen is known as one of the slowest diffusion species in olivine, with a diffusion coefficient more than 4 orders of magnitude slower than Fe or Mg diffusion (*e.g.* Gérard & Jaoul, 1989). Kohlstedt & Mackwell (1998) seem to have definitely abandoned this interpretation in favour of an interpretation based on metal vacancies (V_{Me}).

However, regardless of the species involved, these kinetic data suggest a minimum time for a modification of the concentration of "non-hydrogen point defects" associated with hydrogen following an external change of f_{O_2} and/or a_{opx} (Fig. 5).

Clinopyroxene

The coefficients of self-diffusion in clinopyroxene are much slower than the coefficients of self-diffusion in olivine. For instance, the self-diffusion coefficients of atoms in octahedral sites in diopside (Dimanov & Ingrin, 1995, and Dimanov *et al.*, 1996, for Ca self-diffusion; Freer *et al.*, 1982, and Brady & McCallister, 1983, for Ca-Mg interdiffusion and Fe self-diffusion), are several orders of magnitude slower than diffusion coefficients of atoms from octahedral sites in olivine (Buening & Buseck, 1973; Misener, 1974; Nakamura & Schmalzried, 1984; Hermeling & Schmalzried, 1984; Jurewicz & Watson, 1988; Jaoul *et al.*, 1995).

The diffusion rate of point defects associated with hydrogen incorporation, like V_{Me}, is thus expected to be slower in clinopyroxene than in olivine at the same range of temperatures (DV_{Me} olivine $\approx 10^{-11}$ m²/s at 1100 °C; Fig. 5). Guilhaumou *et al.* (1999) have performed a preliminary experiment on a gem quality Russian diopside single-crystal in order to measure the mobility of the point defects involved in the uptake of hydrogen at 1200 °C (V_{Me}?). The experiment leads to a diffusion coefficient of the order of $5 \cdot 10^{-13}$ m²/s at 1200 °C (Fig. 5) which is assumed to represent the mobility of metal vacancies V_{Me}. This diffusion coefficient is two orders of magnitude lower than that of V_{Me} in San Carlos olivine crystals.

Orthopyroxene and garnet

Despite the lack of diffusion data for orthopyroxene, high-temperature "reequilibration" kinetics similar to that obtained for diopside is expected: the diffusion coefficients of Mg-Fe interdiffusion in orthopyroxene measured from low-temperature experiments (in the range 600-800 °C, E_a = 233 kJ/mole and $D_0 \approx 10^{-9.5}$, Ganguly & Tazzoli, 1992; Brady, 1995) lead by extrapolation to 1100 °C to values close to those for diopside ($\approx 10^{-18}$ m²/s). The kinetics of point defect formation in orthopyroxene is thus expected to be in the same range as for diopside.

The case of pyrope garnet may be somewhat different due to the nature of hydrogen defects. Although substitution of hydrogen in the tetrahedral position by the hydrogarnet substitution $(H_4O_4)^{4-} \Rightarrow SiO_4^{4-}$ may be a mechanism of hydrogen uptake in pyrope (Geiger *et al.*, 1991; Bell & Rossman, 1992b), other incorporation mechanisms which explain the difference of activation energy of diffusion of garnet compared to pyroxenes are acceptable as well. We also notice that diffusion coefficients of Fe and Mg atoms in almandine-pyrope garnets are several orders of magnitude lower than in olivine ($D_{Fe\text{-}Mg}$ and $D_{Mg} \approx 10^{-17}$-10^{-19} m²/s at 1100 °C; Duckworth & Freer, 1981; Cygan & Lasaga, 1985; Elphick *et al.*, 1985; Chakraborty & Ganguly, 1992; Schwandt *et al.*, 1995). We suggest that, like for pyroxenes, the kinetics of reequilibration of the associated "non-hydrogen point defects" (at least partial reequilibration) for pyrope is probably slower than for olivine.

3.3. Geological implications from kinetic data

It is possible, from the kinetic parameters considered above, to determine the time of hydrogen reequilibration of a single crystal as a function of temperature and grain size. We have calculated the time required for olivine, diopside and garnet to reach 95 % of final concentration for a range of grain sizes representative of mantle xenoliths, as shown in Fig. 6 (1-10 mm, see Mercier, 1980). However, this diagram is only semi-quantitative, as numerous data are missing concerning the kinetics of dehydrogenation of garnet, the influence of the iron content on the dehydrogenation kinetics in diopside and the mobility of metal vacancies in pyroxenes. Assuming that the experimental data are directly applicable to mantle conditions several points can be drawn:

For olivine, the fast kinetics of dehydrogenation-hydrogenation suggests that the measured hydrogen content is mainly due to late exchange, which for the smaller crystals may correspond to atmospheric hydrogen loss after eruption, and for the coarser grains to equilibration within a shallow magma chamber. The same remark stands for the hydrogen concentrations measured in mantle pyroxenes and pyrope garnets which, with a similar kinetics of dehydrogenation-hydrogenation (Fig. 4), probably reflect the p_{H_2} conditions prevailing in the last magma reservoir prior to eruption (shallow magma chamber?).

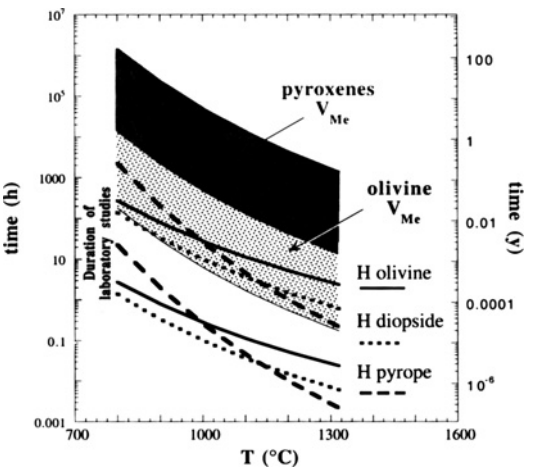

Fig. 6. Time required for 95% reequilibration of H in crystals of 1 to 10 mm size as a function of temperature. Dehydrogenation-hydrogenation reactions of olivine 1 and 10 mm, thick solid curves; pyrope 1 to 10 mm, discontinuous curves; diopside 1 and 10 mm, dotted curves. Partial reequilibration through diffusion of metal vacancies (olivine 1 and 10 mm, dotted area; diopside 1 and 10 mm, grey area). Curves were calculated from the isotropic diffusion parameters (7) given in Ingrin *et al.* (1995) for cubic crystals (2L × 2a × 2b), except for the olivine curves which were deduced from a one-dimensional diffusion relation applied to the [100] direction of olivine (expression (3) in Ingrin *et al.*, 1995).

Thus, the low concentration of hydrogen measured in mantle olivine and garnet compared to pyroxenes from the same origin cannot be explained by a late loss of hydrogen during ascent through the dehydrogenation reaction (1). We think that this difference is better explained by a lower H solubility compared to pyroxenes.

However, the faster mobility of associated point defects in olivine (mainly V''_{Me}) compared to pyroxene may also affect the relative amount of hydrogen preserved in natural samples. The mobility of metal vacancies in olivine is apparently too high to expect that the initial defect concentration of the associated "non-hydrogen point defects" could be completely preserved in olivine in contact with magmas at 900 to 1300 °C. In contrast, with a partial reequilibration time in the range of 1 year at 1100 °C for a crystal of 10 mm, pyroxenes could preserve such information and provide useful data on the thermodynamic condi-

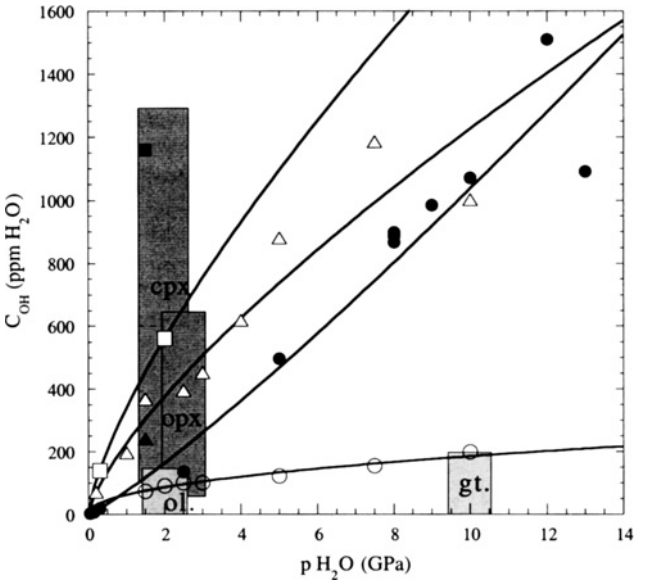

Fig. 7. Compilation of hydrogen solubility data *versus* p_{H_2O} and curve fit by simple power laws of the type $C_{OH} = A \cdot p_{H_2O}^m$. Open circles: pyrope, Lu & Keppler (1997). Filled circles: olivine, Kohlstedt *et al.* (1996). Open triangles: enstatite, Rauch & Keppler (1996). Filled triangle: enstatite, Kohn (1996). Open squares: diopside, Bai *et al.* (1994); Lavie & Ingrin (unpublished data). Filled square: Al-diopside, Kohn (1996). Boxes represent the ranges of hydrogen concentrations of upper-mantle xenoliths as reported in Fig. 2.

tions prevailing in the source regions of some magmas.

We finally remark that, assuming that grain-boundary diffusion of hydrogen is not rate limiting, the kinetics of hydrogen exchange in NAM is so fast that at temperatures prevailing at 410 km depth, equilibrium of hydrous components between the transition zone and the upper part of the upper mantle is quite probable. If no effect of pressure on diffusion coefficients of hydrogen or vacancies is assumed, the characteristic time of diffusion in a 10 mm olivine single crystal at 1500 °C is lower than 1 h and 40 days for hydrogen and vacancies, respectively.

4. Solubility as a function of pressure

Several high-pressure experiments have been recently conducted in order to determine the maximum amount of hydrogen that can be incorporated in olivine, pyroxenes and garnet, and also to determine how the hydrogen concentration in these phases correlate with pressure (total pressure, P, and water fugacity, f_{H_2O}). The maximum amount of hydrogen experimentally incorporated in these phases is on the order of 0.1 wt.% H_2O (1500 ppm for San Carlos olivine, Kohlstedt *et al.*, 1996; 1200 ppm for synthetic enstatite, Rauch & Keppler, 1996; 200 ppm for Dora-Maira pyrope, Lu & Keppler, 1997; 1000 ppm for synthetic pyrope, Withers *et al.*, 1998; about 1160 ppm for diopside, Kohn, 1996). Fig. 7 shows a compilation of the hydrogen solubility at high pressure as a function of total H_2O pressure. We decided to use this raw parameter rather than the H_2O fugacity because the latter quantity is relatively difficult to estimate in several experiments or at least necessitates some restrictive assumptions. However, when H_2O fugacity was relatively well constrained we expressed in the text the dependency of the solubility with this fugacity.

Olivine

Solubility data on San Carlos single-crystal olivine have been collected up to pressure conditions corresponding to the transition zone (Bai & Kohlstedt, 1992; Kohlstedt *et al.*, 1996). Their results suggest that hydrogen solubility, at f_{O_2} conditions controlled by the Ni/NiO buffer, follows the law:

$$C_H = A(T)\, f_{H_2O} \exp(-P\Delta V/RT) \quad (4)$$

with the activation volume $\Delta V = 10.6 \times 10^{-6}$ m^3/mol and $A(T) = 1.1\ H/10^6\ Si\ MPa^{-1}$ for T = 1100 °C, with a maximum solubility at 13 GPa equal to 1510 ppm H_2O. The solubility was deduced from unpolarized FTIR measurements following the calibration of Paterson (1982). The data were extracted from the measurement of the IR absorbance of OH bands between 3780 and 2950 cm^{-1} and represents the contribution from all

different hydrogen defects present in olivine through different OH bands (bands of group I and II, Bai & Kohlstedt, 1993). The solubility measured by Kohlstedt *et al.* (1996) is thus a maximum value, at least in the presence of pure H_2O fluids. However, the Paterson (1982) calibration may underestimate the true amount of hydrogen present in olivine by up to 40 %, if we compare to the new calibration by Libowitzky & Rossman (1997).

The dependence of total pressure (P) on solubility, as proposed by these authors, is difficult to interpret since several types of hydrogen defects are involved: two different defects have indeed been identified in the OH bands from group I, and the bands of group II correspond probably to a third type of defect (see Freund & Oberheuser, 1986; Libowitzky & Beran, 1995).

Clinopyroxene

No systematic studies of the high-pressure solubility of hydrogen in clinopyroxenes have yet been reported, however, the available data indicate that the solubility increases with pressure (*cf.* Fig. 7). At rather moderate conditions, *i.e.* 0.3 GPa and 1100 °C, Bai *et al.* (1994) obtained a solubility of 140 ppm H_2O in single-crystal diopside. In Fe/FeO buffered experiments on polycrystalline diopside performed at 2 GPa and *ca.* 1050 °C, Lavie & Ingrin, unpublished data) obtained a solubility of 560 ppm H_2O. A higher solubility of 1160 ppm H_2O in polycrystalline Al-rich diopside ($Di_{89}CaTs_{11}$) synthesised at 1.5 GPa and 1000-1150 °C was found by Kohn (1996) using ^1H MAS NMR spectroscopy.

Orthopyroxene

Recent experiments performed by Rauch & Keppler (1996; personal comm. 1998) show that up to 1186 ppm H_2O can be incorporated in single-crystal enstatite $MgSiO_3$ in the presence of water at 1100 °C and 7.5 GPa total pressure (Fig. 7). These experiments demonstrate that a large quantity of hydrogen can be stored in enstatite, even without any iron content. This result is consistent with the solubility of 240 ppm H_2O found by Kohn (1996) from ^1H MAS NMR spectroscopy measurements on synthetic polycrystalline enstatite synthesised at 1.5 GPa , 1000-1150 °C (Fig. 7). Furthermore, Rauch & Keppler suggest, similarly to experiments on San Carlos olivine, that a saturation level of the hydrogen concentration occurs above a critical pressure.

Garnet

The same type of experiments as those on olivine and enstatite has been performed on a natural single-crystal pyrope (Dora-Maira) by Lu & Keppler (1997), in piston cylinder and multi-anvil apparatus with Ni/NiO buffer and pressures up to 10 GPa. Lu & Keppler (1997) succeeded to incorporate up to 100 and 200 ppm H_2O in pyrope at 3 and 10 GPa, respectively. For comparison the amounts incorporated in olivine or enstatite are 200 and 450 ppm H_2O respectively at 3 GPa and around 1000 and 1200 ppm H_2O at 10 GPa (see Fig. 7).

Withers *et al.* (1998) have crystallised synthetic pyrope crystals with up to 1000 ppm H_2O as hydrogarnet defects, at 1000 °C and 5 GPa in the presence of excess SiO_2. The authors show that above 7 GPa only anhydrous pyrope crystallised in their experiments, suggesting that the stability field of hydrogarnet defects is relatively narrow in the upper mantle. However, comparison of these results with the data from Lu & Keppler (1997) or with the hydrogen concentration measured in natural garnet xenoliths is rather difficult as the nature of hydrogen defects in the latter garnets is different. Thus, the IR absorption peak reported in crystallised synthetic pyrope is centred at 3630 cm^{-1} while this peak is almost absent in natural pyropes (main peaks are centred at 3670 cm^{-1} and 3570 cm^{-1} in natural samples; see Bell & Rossman, 1992b; Bell *et al.*, 1995; Wang *et al.*, 1996).

General comments

It is clear from the results of the above-mentioned hydrogen solubility experiments that a maximum average concentration in the range of 1000 ppm H_2O may be stored in upper-mantle NAM, at saturated mantle conditions, at least in the main phases: olivine and pyroxenes. However, the water saturation condition for the entire mantle above 410 km is not realistic. The solubility data collected are still preliminary; for instance, the effect of the composition of mineral phases on the hydrogen solubility has not yet been addressed and data have so far only been collected for restricted f_{O_2} conditions (mainly under Ni/NiO buffer).

However, in a first attempt to understand hydrogen storage in the upper mantle, we may assume that the above data are representative of the solubility dependence of H in mantle phases with pressure.

Except for pyrope, the maximum amount of hydrogen measured in natural upper-mantle NAM corresponds roughly to the range of solubility obtained experimentally for a total water pressure of 1 to 3 GPa (*cf.* Fig. 2 and Fig. 7). The amount of hydrogen incorporated experimentally in diopside, enstatite and olivine, shows the same range of concentrations as those observed in nature, suggesting that the differences of concentration observed in natural xenoliths are largely caused by a true difference of H solubility in NAM and not only due to a difference of kinetics of reequilibration.

The minimum contents of hydrogen present in pyroxenes from upper-mantle xenoliths (around 60 and 100 ppm H_2O for opx and cpx, respectively) correspond to the solubility at a p_{H_2O} lower than 0.2 GPa for both minerals. For the same p_{H_2O}, the amount of hydrogen that can be incorporated in olivine and pyrope is lower than 10-20 ppm H_2O. These low concentrations may reflect late-stage hydrogen equilibration of the xenoliths with the host continental alkali basalt, kimberlite, or island arc magma from which they were extracted. The minimum hydrogen contents observed in xenolith samples could thus correspond to their solubility at the low p_{H_2O} conditions prevailing in the host magmas at shallow depths.

The apparent difference in behaviour of garnet, with a maximum solubility in xenoliths corresponding to equilibrium with a p_{H_2O} of 10 GPa (Fig. 7), may have two reasons. Firstly, Dora-Maira pyropes used for the experimental study of Lu & Keppler (1997) show very sharp OH bands unlike the majority of natural pyropes, which indicates that the Dora-Maira pyrope may not be fully representative for mantle garnets. Secondly, the kinetics of reequilibration of pyrope garnets (reaction involving host defects, see chapter 3) may be much slower than reequilibration in olivine or even in pyroxenes, and thus may preserve information from deeper levels than the other minerals (as suggested by the measurements on mantle garnets by Bell & Rossman, 1992b).

The most recent solubility measurements show the occurrence of a H saturation level at high pressures (Kohlstedt *et al.*, 1996; Rauch & Keppler, 1996; Withers *et al.*, 1998). The authors generally explain this behaviour by an activation volume, ΔV, which is related to the volume change of the mineral lattice upon hydrogenation. The expressions of the solubility suggest that a decrease of solubility should occur at high water fugacity, and some data support this possibility (Kohlstedt *et al.*, 1996; Rauch & Keppler, 1996; Withers *et al.*, 1998). However, this has not yet been clearly proved for all types of hydrogen defects as all the reactions of hydrogen incorporation involved in the process are not yet clearly elucidated, and the occurrence of a decrease in hydrogen solubility in upper mantle NAM is still questionable.

The most important conclusions derived from the experimental results on hydrogen solubility can be summarised as follow. The minimum amount of hydrogen stored in mantle xenolith samples corresponds roughly to the saturation conditions of pH_2O prevailing in shallow magma chambers, with the occasional exception of olivine that sometimes contains only sub-ppm concentrations of hydrogen (*e.g.* Miller *et al.*, 1987). The presence of numerous xenoliths with higher H concentrations (*e.g.* Bell & Rossman, 1992a) suggests that these xenoliths probably have been in contact with higher pH_2O conditions in deeper parts of the upper mantle, and that they have kept a memory of those (Bell *et al.*, 1994). If, during their transport toward the surface, some xenoliths have crossed a mantle region dryer than the concentration corresponding to the condition of a shallow magma chamber, they are likely to have kept a memory also of that. Thus it is reasonable to assume that such hydrogen-poor regions of the mantle do not exist, and that the average hydrogen concentration of the upper mantle above 410 km depth is higher than this limit (around 60 to 100 ppm H_2O for pyroxenes).

5. Implications from the Fe^{3+} contents of xenolith samples

As previously mentioned, a major question in estimating the actual hydrogen concentration in NAM within the upper mantle is whether the hydrogen concentrations measured in mantle xenoliths are representative for the mantle conditions, or if hydrogen has been lost (or gained) during the ascent process. If hydrogen has been lost by the dehydrogenation-oxidation reaction (1), which appears as the fastest hydrogen exchange process, a corresponding increase in the ferric iron contents

Table 3. Ferric iron content and possible hydrogen loss for nominally anhydrous mantle minerals.

Mineral	Fe_2O_3 Wt.%	max H_2O loss ppm H_2O	H_2O_{meas} ppm H_2O	Ref.
clinopyroxene	0.40 - 0.80	450 - 900	100 - 1080	[1], [2]
orthopyroxene	0.29 - 0.50	320 - 570	60 - 450	[1], [2]
olivine	< 0.22	250	0.1 - 140	[1]
garnet	0.13 - 1.57	150 - 1800	1 - 200	[3]

Ferric iron data from [1], Dyar *et al.* (1989); [2], Luth & Canil (1993); [3], Luth *et al.* (1990).

of the different minerals should be expected. Comparisons can be made with mantle-derived amphiboles.

In a study based on 16 kaersutite samples obtained from hornblende megacrysts in basaltic flows, Dyar *et al.* (1992) found an inverse correlation of the hydrogen and ferric iron concentrations. The correlation was interpreted as evidence for hydrogen loss in connection with iron oxidation during the ascent process. Without knowledge of the initial ferric iron contents in NAM in the upper mantle, an eventual increase can of course not be determined. Data on both the hydrogen and ferric iron contents in NAM from the upper mantle would be valuable, but are unfortunately not available. Nevertheless, the total ferric iron contents will provide an estimate of the maximum possible amount of hydrogen that may have been lost by the dehydrogenation-oxidation reaction. Hence it may be worthwhile to consider the ferric iron contents of the most important NAM.

Fe^{3+} concentrations

The oxidation state of iron in mantle-derived clino- and orthopyroxene has been investigated by Mössbauer spectroscopy. For clinopyroxene, Dyar *et al.* (1989) report Fe^{3+}/Fe^{tot} values in the range 0.12-0.23 for five spinel lherzolite samples, and Luth & Canil (1993) report values in the similar range of 0.12-0.24 for ten samples, also of spinel-lherzolite origin. Assuming a nominal total Fe content of 3 wt.% FeO for this type of samples, the ratios correspond to a ferric iron concentration of 0.40-0.80 wt.% Fe_2O_3, and a corresponding maximum hydrogen loss for clinopyroxene in the range 450-900 ppm H_2O (Table 3). For orthopyroxene, the same authors report Fe^{3+}/Fe^{tot} values in the range 0.04-0.07 (with one outlier at 0.14) for 12 samples of the same origin. These lower ratios are compensated by the higher total Fe contents in orthopyroxene, with a mean value of 6.5 wt.% FeO, resulting in a comparable ferric iron concentration of 0.29-0.50 wt.%. The maximum hydrogen loss for orthopyroxene is thus limited to 320-570 ppm H_2O (Table 3).

The ferric iron content in mantle-derived garnets has been investigated by Luth *et al.* (1990). Mössbauer data obtained on 23 samples from mantle xenoliths show a bimodal distribution with garnets from low-temperature garnet lherzolites having $Fe^{3+}/Fe^{tot} < 0.07$ whereas samples from high-temperature garnet lherzolites have $Fe^{3+}/Fe^{tot} > 0.10$. The ferric iron concentration is in the range 0.13-1.57 wt.% Fe_2O_3, which sets an upper limit of possible hydrogen loss in the interval 150-1800 ppm H_2O for the different samples (Table 3).

Olivine shows considerably lower Fe^{3+}/Fe^{tot} values, but it has not been possible to detect ferric iron in mantle olivine by Mössbauer spectroscopy at all (*e.g.* Dyar *et al.*, 1989). Assuming a detection level around 0.02 in Fe^{3+}/Fe^{tot}, together with a total iron content of 10 wt.% FeO, the ferric iron content should be below 0.2 wt.% Fe_2O_3. This corresponds to a maximum possible loss of hydrogen of 250 ppm H_2O (Table 3).

Limitations of hydrogen loss

The highest possible amounts of hydrogen that may have been lost by the dehydrogenation-oxidation reaction in olivine, clino- and orthopyroxene are comparable to the upper ranges of reported hydrogen concentrations for the different minerals (Table 3). These values of possible hydrogen loss represent upper limits since the

phases, with the possible exception of olivine, cannot be considered devoid of ferric iron in the upper mantle (*e.g.* O'Neill *et al.*, 1993).

The much higher hydrogen concentrations that have been reported for olivine from solubility experiments at high p_{H_2O} (Kohlstedt *et al.*, 1996; Fig. 7) seem not representative for the upper mantle. If such high concentrations were present in olivine in the upper mantle, and then decreased during ascent by the dehydrogenation-oxidation reaction to the low levels that are measured, around one order of magnitude higher ferric iron contents should be expected. However, the comparatively fast kinetics of reactions involving the formation of vacancy point defects in olivine (*cf.* reaction 3) may have allowed reequilibration and loss of hydrogen by reactions which do not change the ferric iron content. Two models of hydrogen loss appear possible considering the experimental data.

1) Olivine xenoliths may initially contain around 100 ppm H_2O. During the ascent, varying amounts of H_2O are lost according to the oxidation-dehydrogenation reaction (1), leading to the observed range of 0-100 ppm H_2O. The equivalent amounts of Fe^{3+} are produced, but the low concentrations cannot be detected analytically. The range in dehydrogenation may be caused by different conditions during the ascent process.

2) Olivine xenoliths lose hydrogen by a combination of reactions (1) and (3), leading to the observed range of 0-100 ppm H_2O. No extra Fe^{3+} is produced in this process following for instance the equation (3) + (1) :

$$Me_{Me}^{x} + H_2O = (2H)_{Me}^{x} + MeO. \quad (4)$$

In the latter model, the initial hydrogen contents cannot be deduced from the Fe^{3+}/Fe^{tot} ratio.

Garnet seems to be the only case of the considered phases that has such a high ferric iron concentration that major dehydrogenation by the dehydrogenation-oxidation reaction cannot be ruled out (Table 3). The maximum ferric iron concentration corresponds to hydrogen loss around 10-20 times higher than what is normally measured in mantle garnets. This implies that dehydrogenation is not limited by the ferric iron content, and may have occurred to a substantial degree. On the other hand, published solubility data show that the solubility in pyrope-rich garnets is not very high (Lu & Keppler, 1997; Fig. 7), except for the hydrogarnet defect (Withers *et al.*, 1998). Although not strictly comparable, it is worth noting that garnets from high-temperature peridotites in South Africa have been reported to have higher H_2O contents than samples from low-temperature peridotites (Bell & Rossman, 1992b), whereas samples from high-temperature garnet lherzolites have higher Fe^{3+} contents than samples from low-temperature garnet lherzolites (Luth *et al.*, 1990). Thus the negative correlation of hydrogen and ferric iron concentration (expected, if a notable amount of dehydrogenation occurred through reaction (1) during ascent) is not confirmed in the mantle garnets.

In view of the reported ferric iron contents, it seems that the initial hydrogen concentrations in upper-mantle clino- and orthopyroxene may be around two times higher than the actually observed upper values, *i.e.* 1000 ppm H_2O for ortho- and 2000 ppm H_2O for clinopyroxene. These values represent maximum levels, if we assume that hydrogen exchange occurs only through reaction (1) since the diffusion kinetics of associated non-hydrogen defects in clino- and orthopyroxene are relatively slow. Compared with the available solubility data (*cf.* Fig. 7), these hydrogen concentrations correspond to equilibrium p_{H_2O} of less than 10 GPa for both minerals.

Oxidation-dehydrogenation processes in mantle xenoliths during ascent may also have important implications for models concerning the oxidation state of the mantle (cf. Luth & Canil, 1993; O'Neill *et al.*, 1993). When such models are based on Fe^{3+}/Fe^{tot} ratios obtained on mantle minerals that may have lost hydrogen during the ascent process, it should be taken into account that the initial Fe^{3+}/Fe^{tot} ratios may not necessarily be preserved during the ascent process, and that the actual ratios in the mantle could be significantly different. Concomitant measurements of the hydrogen contents and the Fe^{3+}/Fe^{tot} ratios in mantle minerals should be valuable in constraining these oxidation-state models.

6. Constraints on the water solubility in the upper mantle

6.1. Solubility limits at water-saturation conditions

As mentioned earlier, it is not justified to imagine that minerals in the entire upper mantle could be saturated with water stored as hydrogen-bearing defects. However, we know that at depths between 100 and 200 km, subducted lithospheric oceanic

plates dehydrate and release a relatively large amount of water to the upper mantle wedge above the slab (Thompson, 1992; Bell & Rossman, 1992a). It is thus realistic to assume that this mantle wedge may be water-saturated with a total p_{H_2O} of 3 to 6 GPa, similar to the conditions of the solubility experiments, assuming that no important contributions from other volatile phases are present (*e.g.* CO_2).

With the assumption that the experimental solubility data (Fig. 7) are directly applicable to upper-mantle conditions, it is possible to estimate the maximum amount of H present in NAM in this water-rich region at 150 km depth. The maximum water content is approximately 520 ppm H_2O if we assume a garnet-peridotite mantle and a mineralogical model composed of 0.66 olivine + 0.27 opx + 0.03 cpx + 0.04 garnet (McDonough, 1990). This water content can reach around 610 ppm H_2O if, as indicated by the new calibration of Libowitzky & Rossman (1997), an underestimation of 40 % is assumed on the hydrogen-solubility measurements in olivine.

In the shallow oceanic lithospheric mantle below 3 GPa (above 100 km), the maximum expected hydrogen content at p_{H_2O} saturation in spinel peridotite composed of 0.62 olivine + 0.24 opx + 0.12 cpx (McDonough, 1990) reaches about 370 ppm H_2O (435 ppm H_2O for a 40 % underestimation on olivine). Thus, a concentration of 600 ppm H_2O is considered an upper limit in the upper mantle, at least above 150 km depth.

6.2. Constraints from the water content of melts

Previous attempts to determine the amount of water in the upper mantle were essentially based on measurements of the water content of quenched matrix glass of pillow lava or glass inclusions present in phenocrysts from mid-ocean ridge basalts (MORB) and subduction-zone magmas (*e.g.* Michael, 1988; Dixon *et al.*, 1988; Jambon & Zimmermann, 1990; Sisson & Layne, 1993; Danyushevsky *et al.*, 1993; Sobolev & Chaussidon, 1996). The average concentrations measured in the most primitive magmas range from 0.1 to 0.5 wt.% H_2O for MORB and 1.0 to 2.9 wt.% H_2O for subduction related magmas (Sobolev & Chaussidon, 1996).

Almost all of these authors assume a partition coefficient for H_2O between minerals and melt (D^w) around 0.01. They deduce the H_2O concentration in the source region from the estimate of the fraction of partial melting (around 5 to 20 %). For N-MORB or intermediate T-MORB sources the water contents range from 60 to 300 ppm H_2O. For E-MORB the concentration may be higher, with 200 to 950 ppm H_2O. For subduction zones the amount is much higher with 600 to 1900 ppm H_2O for 5 % partial melting. The difference in concentration inferred from aggregated fractional melting and batch melting model is not really significant (Sobolev & Chaussidon, 1996).

Before the possibility of water storage in NAM was considered, the amount of water in the shallow upper mantle was interpreted as evidence for the presence of hydrous minerals or water-rich fluids in the source regions of magma (Michael, 1988; Dixon *et al.*, 1988; Jambon & Zimmermann, 1990; Sisson & Layne, 1993; Danyushevsky *et al.*, 1993). The water concentrations deduced from MORB are not in contradiction with the water contents in NAM as deduced from the saturation experiments, and the presence of hydrous minerals is hence not systematically required in the source region. On the other hand, water-saturation conditions in NAM seem not sufficient to explain the concentration of 600 to 1900 ppm H_2O derived from subduction zone magmas.

However, all these estimations from basalt water content are based on assumptions that may be problematic.

1) For instance, it is generally assumed that the partition coefficient of water (D^w) between mineral residue and melt during partial melting is equal to 0.01. This assumption has been deduced from the similarity of the behaviour of water and La partitioning (Dixon *et al.*, 1988). However, the two so far reported partition coefficients of water between NAM and melt measured on natural samples lead to different results. Kurosawa *et al.* (1997) observed a D^w of 0.015 between olivine and glass inclusions from ion-probe measurements, and Dobson *et al.* (1995) measured a partition coefficient between orthopyroxene and boninite glasses in the range 0.003-0.004 from IR analyses. The latter data should be shifted to 0.001-0.002 if the new calibration on IR data for hydrogen in orthopyroxene of Bell *et al.* (1995) is applied. Considering the larger hydrogen solubility in enstatite compared to olivine, the final partition coefficient between melt and upper-mantle peridotites deduced from these data should be 0.02 and 0.001 respectively. If we assume that

the partition coefficient is equal to 0.001 and that no hydrous phase is present in the source magma of subduction-related volcanoes (Sobolev & Chaussidon, 1996), the expected amount of water estimated for 5 % fractional melting is reduced to the range 500-1500 ppm H_2O. An experimental determination of the partition coefficient as well as the identification of the parameters that may affect the distribution are highly needed in order to propose a firm estimation of the water content in the upper mantle.

2) The models applied by a majority of the authors assume that hydrogen partitioning between melt and upper-mantle minerals is governed by equilibrium partial melting. The role played by equilibrium partial melting in MORB and subduction-zone magma genesis has been questioned several times (Bédard, 1989; Qin, 1992; Iwamori, 1993). Disequilibrium partial melting is directly related to the rate of diffusion of the relevant elements in minerals compared to the rate of the upward migration of the melt. If diffusion rates of species are very different, as is expected for the diffusion of hydrogen and lanthanum in minerals, a direct relation between elements correlation and partition coefficients cannot be assumed.

3) Furthermore, the uncertainty on the fraction of melting is quite large, and especially difficult to estimate if disequilibrium partial melting occurs. For instance, partial melting between 6 and 2 % is sufficient to explain 1.0 to 2.9 wt.% H_2O in glass inclusions, assuming a partition coefficient between melt and NAM equal to 0.001. The presence of hydrous phases in the magma source regions cannot be excluded, but exchange between melt and NAM must also be considered and the partition coefficient between NAM and melt must be measured with sufficient accuracy.

Nevertheless, the available data on hydrogen solubility in NAM from natural samples and from laboratory experiments suggest that the average concentration of hydrogen in the upper mantle above the transition zone range from a minimum value of about 30 ppm H_2O to a maximum limit that should not be much higher than 600 ppm H_2O. We have seen in a previous section that hydrogen exchange in NAM can be very fast, faster than the normal rate of material transport through mantle convection. The mantle wedge above the subduction zone at 150 km depth is one of the "wettest" parts of the upper mantle above 410 km depth, and the hydrogen concentration of NAM in this region is probably close to the saturation level. These observations are in accordance with an average hydrogen concentration in upper mantle NAM closer to the 600 ppm H_2O upper value than to 30 ppm H_2O.

6.3. Connections with the transition zone

The estimation of the amount of hydrogen stored in the upper mantle above 410 km is a key question if we want to constrain the amount of water stored in the transition zone between 410 and 660 km depth. Recent experimental results have shown that β-$(Mg,Fe)_2SiO_4$ can incorporate up to 3.3 wt.% H_2O, suggesting that the transition zone is probably the main water reservoir of the upper mantle (Smyth, 1987, 1994; McMillan *et al.*, 1991; Inoue *et al.*, 1995; Kudoh *et al.*, 1996). Experimental estimates of the partition coefficient of water between olivine, α-$(Mg,Fe)_2SiO_4$, and wadsleyite, β-$(Mg,Fe)_2SiO_4$, give values around $D^{\alpha/\beta}$ = 1/40 (Young *et al.*, 1993) and $D^{\alpha/\beta}$ = 1/20 (Kohlstedt *et al.*, 1996). All laboratory experiments performed on these phases show that the amount of water stored in wadsleyite is at least ten times higher than in olivine. According to these observations Wood (1995) proposed to constrain the amount of water in the upper mantle from the effect of water on the width of the α-β binary phase loop. Assuming a partition coefficient $D^{\alpha/\beta}$ of 1/10 and a maximum thickness of the 410 km seismic discontinuity of 13 km, Wood (1995) concludes from thermodynamic considerations that H_2O concentration of 200 ppm is an upper limit for the upper mantle above 410 km.

However, according to Stixrude (1997), the presence of pyroxenes and garnet, not considered in Wood's model, may substantially narrow the width of the binary phase loop and could partly compensate the effect of water. Wood's model predicts a very wide phase-boundary loop for high concentration of water in olivine, wider than 1.5 GPa at 1500 °C for an olivine concentration of 1200 ppm H_2O, and even more if a lower $D^{\alpha/\beta}$ is applied. For comparison, experiments performed by Kohlstedt *et al.* (1996) with the same amount of water at 1100 °C show that the width of the loop is narrower than 1 GPa (between 13 and 14 GPa, in agreement with previous dry experiments; Katsura & Ito, 1989; Fei *et al.*, 1991). However, to our knowledge, no experimental evidence for a notable increase of the width of the olivine-wad-

sleyite transition in the presence of water has been published.

The kinetics of hydrogen exchange between NAM is fast enough (see section 3) to assume that the transition zone is probably in equilibrium with the upper part of the upper mantle. From the expected range of water contents in the olivine stability field of the upper mantle (30-600 ppm H_2O), and the available data on the partition coefficient between olivine and wadsleyite, we can estimate the amount of water included in the wadsleyite phase of the transition zone to 0.06-1.8 wt.% H_2O. These values compare favourably with the recent estimation of 1-2 wt.% H_2O by Yusa & Inoue (1997) from compressibility data of hydrous wadsleyite.

7. Conclusions and perspectives

Conclusions

Estimating the amount of hydrogen stored in the upper mantle above 410 km is a complex problem which needs to be adressed in order to quantify the water cycle in the Earth's interior. Much progress has been achieved during the past ten years in the understanding of water storage in the upper mantle. In particular, storage of hydrogen in NAM is now well established and is no longer the research field of mineralogists only. Hydrogen has been found in most NAM from the upper mantle, with decreasing concentration of hydrogen following the mineral series diopside > enstatite > pyrope > olivine. The nature of the point defects involved in the process of hydrogen uptake in these minerals has been elucidated, even if not completely clarified. In particular for pyroxenes and olivine we know that protons, as well as Fe^{3+}, play a key role in the process of charge compensation correlated with point defects such as cations vacancies and heterovalent substitutions. Kinetic studies have shown that both Fe^{3+} and H^+ are involved at low temperatures in the reaction of hydrogenation-dehydrogenation following reaction (1):

$$Fe^{3+} + O^{2-} + 1/2\ H_2 = Fe^{2+} + OH^- \qquad (1)$$

The kinetics of this reaction has been shown to be so fast for pyroxenes, olivine and pyrope, that we assume that numerous mantle xenolith samples loose a part of their initial hydrogen content during ascent from the mantle.

Olivine has also a fast kinetics of creation-annihilation of point defects associated with hydrogen storage (mainly vacancies) suggesting that this mineral may have lost or gained some of these defects, following a reaction as expressed by (3):

$$2\ Fe_{Me}^{x} + Me_{Me}^{x} + 1/2\ O_2 = 2\ Fe_{Me}^{\bullet} + V_{Me}'' + MeO \qquad (3)$$

However, the substantially slower kinetics of this reaction for pyroxenes, and probably pyrope, suggests that these minerals are able to preserve a part of the concentration of point defects they inherited from their upper-mantle source region.

The recent high-pressure experiments performed in order to measure the solubility of hydrogen in these minerals largely confirm the trend observed in natural samples: at the same p_{H_2O} hydrogen solubilities decrease in the mineral series from diopside > enstatite > olivine > pyrope.

As confirmed by the reactions discussed above, the concentrations of Fe^{3+} and H^+ are clearly related and the amount of Fe^{3+} measured in the upper-mantle xenolith samples is of the same range as the hydrogen content (except for pyrope). It suggests that the concentrations of the two cations in the upper mantle are highly dependent, and their behaviour cannot be studied independently. The average concentration of hydrogen in upper mantle NAM, as deduced from the present knowledge from natural samples and experimental results, is somewhere between 30 and 600 ppm H_2O, probably closer to the upper limit.

Perspectives

An error of 100 ppm H_2O in the determination of the amount of hydrogen stored in NAM of the upper mantle above 410 km may drastically change the results of net budget calculations of the Earth's internal water cycle: an extra amount of 100 ppm H_2O in this upper part of the upper mantle is equivalent to an extra 100 m water layer at the Earth's surface, and increases the amount of water in the transition zone by at least 1000 ppm H_2O (assuming that $D^{\alpha/\beta} = 1/20$).

In the future, the problem of water storage in the upper mantle will be accurately solved only if we are able to accomplish the following tasks:

- determine the different types and locations of hydrogen defects in diopside, enstatite, olivine and pyrope;

- further develop quantitative methods (IR, ion probe, nuclear reaction analysis, NMR, *etc.*) to measure the concentration of hydrogen in small upper-mantle samples;
- determine the dependence of hydrogen solubility on mineral composition and oxygen fugacity;
- accurately measure the partition coefficients of hydrogen between NAM and melt;
- determine the kinetics of the involved reactions and the hierarchy of these kinetics for the four types of minerals;
- perform systematic studies of the relation between Fe^{3+} and hydrogen content in mantle xenoliths.

Acknowledgements: We wish to thank Simon C. Kohn and Anton Beran for their helpful discussions and comments on an early version of the manuscript. We acknowledge the valuable review and comments of C. Chopin, E.A. Johnson, E. Libowitzky and G.R. Rossman. This work was supported by grants from the International committee CNRS and the Swedish National Science Research Council (NFR). This is CNRS-INSU contribution # 185, programme 97 IT 62.

References

Ackermann, L., Cemic, L., Langer, K. (1983): Hydrogarnet substitution in pyrope: a possible location for "water" in the mantle. *Earth Planet. Sci. Lett.*, **62**, 208-214.

Aines, R.D. & Rossman, G.R. (1984a): Water in minerals? A peak in the infrared. *J. Geophys. Res.*, **89**, 4059-4071.

– – (1984b): The water content of mantle garnets. *Geology*, **12**, 720-723.

– – (1984c): The hydrous component in garnets: pyralspites. *Am. Mineral.*, **69**, 1116-1126.

Bai, Q. & Kohlstedt, D.L. (1992): Substantial hydrogen solubility in olivine and implications for water storage in the mantle. *Nature*, **357**, 672-674.

– – (1993): Effect of chemical environment on the solubility and incorporation mechanism for hydrogen in olivine. *Phys. Chem. Minerals*, **19**, 460-471.

Bai, Q., Wang, Z.C., Dresen, G., Mei, S., Kohlstedt, D.L. (1994): Solubility and stability of hydrogen in diopside single crystals. *EOS*, **75**, 652.

Barnes, V.E. (1930): Changes in hornblende at about 800 °C. *Am. Mineral.*, **15**, 393-417.

Bédard, J.H. (1989): Disequilibrium mantle melting. *Earth Planet. Sci. Lett.*, **91**, 359-366.

Bell, D.R., Ihinger, P.D., Rossman, G.R. (1995): Quantitative analysis of trace OH in garnet and pyroxenes. *Am. Mineral.*, **80**, 465-474.

Bell, D.R. & Rossman, G.R. (1992a): Water in Earth's mantle: The role of nominally anhydrous minerals. *Science*, **255**, 1391-1397.

– – (1992b): The distribution of hydroxyl in garnets from the subcontinental mantle of southern Africa. *Contrib. Mineral. Petrol.*, **111**, 161-178.

Bell, D.R., Rossman, G.R., Endish, D., Rauch, F. (1994): OH content of mantle olivine. *EOS*, **75**, 230.

Behrens, H. (1994): Structural, kinetic and thermodynamic properties of hydrogen in feldspars. *in* Proceedings of a E.S.F. workshop on: Kinetics of cation ordering, Putnis, A., Ed., Cambridge, 1-7.

Beran, A. (1976): Messung des Ultrarot-Pleochroismus von Mineralen. XIV. Der Pleochroismus der OH-Streckfrequenz in Diopsid. *Tscherm. Min. Petr. Mitt.*, **23**, 79-85.

Beran, A. & Putnis, A. (1983): A model of the OH positions in olivine, derived from infrared-spectroscopic investigations. *Phys. Chem. Minerals*, **9**, 57-60.

Beran, A. & Zemann, J. (1986): The pleochroism of a gem-quality enstatite in the region of the OH stretching frequency, with a stereo chemical interpretation. *Tscherm. Min. Petr. Mitt.*, **35**, 19-25.

Brady, J.B. (1995): Diffusion data for silicate minerals, glasses, and liquids. *in* "Mineral Physics & Crystallography: A handbook of physical constants", Ahrens, T.J., Ed., American Geophysical Union reference shelf 2, Washington, 269-290.

Brady, J.B. & McCallister, R.H. (1983): Diffusion data for clinopyroxenes from homogenization and self-diffusion experiments. *Am. Mineral.*, **68**, 95-105.

Buening, D.K. & Buseck, P.R. (1973): Fe-Mg lattice diffusion in olivine. *J. Geophys. Res.*, **78**, 6852-6862.

Carpenter, S.J. (1996): The kinetics of hydrogen diffusion in single crystal clinopyroxene. 81 p., Master thesis, Pennsylvania State University, USA.

Carpenter, S.J., Mackwell, S.J., Dyar, M.D. (2000): Hydrogen in diopside diffusion profiles. *Am. Mineral.*, **85**, 480-488.

Chakraborty, S. & Ganguly, J. (1992): Cation diffusion in aluminosilicate garnets: Experimental determination in spessartine-almandine diffusion couples, evaluation of effective binary diffusion coefficients, and applications. *Contrib. Mineral. Petrol.*, **111**, 74-86.

Chen, J., Inoue, T., Weidner, Y.W., Vaughan, M.T. (1998): Strength and water weakening of mantle minerals, olivine, wadsleyite and ringwoodite. *Geophys. Res. Lett.*, **25**, 575-578.

Cho, H. & Rossman, G.R. (1993): Single-crystal NMR studies of low-concentration hydrous species in minerals: Grossular garnet. *Am. Mineral.*, **78**, 1149-1164.

Chopra, P. & Paterson, M.S. (1984): The role of water in the deformation of dunite. *J. Geophys. Res.*, **89**, 7861-7876.

Clowe, C.A., Popp, R.K., Fritz, S.J. (1988): Experimental investigation of the effect of oxygen fugacity on ferric-ferrous ratios and unit-cell parameters of four natural clinoamphiboles. *Am. Mineral.*, **73**, 487-499.

Cygan, R.T. & Lasaga, A.C. (1985): Self-diffusion of magnesium in garnet at 750° to 900 °C. *Am. J. Sci.*, **285**, 328-350.

Danyushevsky, L.V., Falloon, T.J., Sobolev, A.V., Crawford, A.J., Carroll, M., Price, R.C. (1993): The H_2O content of basalt glasses from Southwest Pacific back-arc basins. *Earth Planet. Sci. Lett.*, **117**, 347-362.

Dimanov, A. & Ingrin, J. (1995): Premelting and high-temperature diffusion of Ca in synthetic diopside: An increase of the cation mobility. *Phys. Chem. Minerals*, **22**, 437-442.

Dimanov, A., Jaoul, O., Sautter, V. (1996): Calcium self-diffusion in natural diopside single crystals. *Geochim. Cosmochim. Acta*, **60**, 4095-4106.

Dixon, J.E., Stolper, E.M., Delaney, J.R. (1988): Infrared spectroscopic measurements of CO_2 and H_2O in Juan de Fuca Ridge basaltic glasses. *Earth Planet. Sci. Lett.*, **90**, 87-104.

Dobson, P.F., Skogby, H., Rossman, G.R. (1995): Water in boninite and coexisting orthopyroxene: concentration and partitioning. *Contrib. Mineral. Petrol.*, **118**, 414-419.

Drury, M.R. (1991): Hydration-induced climb dissociation of dislocations in naturally deformed mantle olivine. *Phys. Chem. Minerals*, **18**, 106-116.

Duckworth, S. & Freer, R. (1981): Cation diffusion studies in garnet-garnet and garnet-pyroxene couples at high temperatures and pressures. *in* "Fifth Progress Report of Research Supported by Natural Environment Research Council (1978-1980)", **18**, 36-39.

Dyar, M.D., Mackwell, S.J., McGuire, A.V., Cross, L.R., Robertson, J.D. (1993): Crystal chemistry of Fe^{3+} and H^+ in mantle kaersutite: Implications for mantle metasomatism. *Am. Mineral.*, **78**, 938-979.

Dyar, M.D., McGuire, A.V., Mackwell, S.J. (1992): Fe^{3+}/H^+ and D/H in kaersutites - Misleading indicators of mantle source fugacities. *Geology*, **20**, 565-568.

Dyar, M.D., McGuire, A.V., Ziegler, R.D. (1989): Redox equilibria and crystal chemistry of coexisting minerals from spinel lherzolite mantle xenoliths. *Am. Mineral.*, **74**, 969-980.

Elphick, S.C., Ganguly, J., Loomis, T.P. (1985): Experimental determination of cation diffusivities in aluminosilicate garnets: I. Experimental methods and interdiffusion data. *Contrib. Mineral. Petrol.*, **90**, 36-44.

Ernst, W.G. & Wai, C.M. (1970): Infrared, X-ray and optical study of cations ordering and dehydrogenation in natural and heat-treated sodic amphibole. *Am. Mineral.*, **55**, 1226-1258.

Fei, Y., Mao, H.K., Mysen, B O. (1991): Experimental determination of element partitioning and calculation of phase relations in the MgO-FeO-SiO_2 system at high pressure and high temperature. *J. Geophys. Res.*, **96**, 2157-2169.

Freer, R., Carpenter, M.A., Long, J.V.P., Reed, S.J.B. (1982): "Null result" diffusion experiments with diopside: implications for pyroxene equilibria. *Earth Planet. Sci. Lett.*, **58**, 285-292.

Freund, F. & Oberheuser, G. (1986): Water dissolved in olivine: A single-crystal infrared study. *J. Geophys. Res.*, **91**, 745-761.

Gaetani, G.A., Grove, T.L., Bryan, W.B. (1993): The influence of water on the petrogenesis of subduction related igneous rocks. *Nature*, **365**, 332-334.

Ganguly, J. & Tazzoli, V. (1992): Fe^{2+}-Mg interdiffusion in orthopyroxene: constraints from cation ordering and structural data and implications for cooling rates of meteorites (abstract). *in* "Lunar and Planet. Science XXIV", Lunar and Planet. Institute, Houston, 517-518.

Gasparik, T. (1986): Experimental study of subsolidus phase relations and mixing properties of clinopyroxene in the silica-saturated system CaO-MgO-Al_2O_3-SiO_2. *Am. Mineral.*, **71**, 686-693.

Geiger, C.A., Langer, K., Bell, D.R., Rossman, G.R., Winkler, B. (1991): The hydroxide component in synthetic pyrope. *Am. Mineral.*, **76**, 49-59.

Gérard, O. & Jaoul, O. (1989): Oxygen diffusion in San Carlos olivine. *J. Geophys. Res.*, **94**, 4119-4128.

Guilhaumou, N., Dumas, P., Ingrin, J., Carr, G.L., Williams, G.P. (1999): Microanalysis of fluids in minerals in the micron scale range by synchrotron infrared microspectrometry. *Internet J. Vibrational Spectro.* [www.ijvs.com], **3**, 1, 11.

Hawthorne, F.C. (1981): Crystal chemistry of amphiboles. Mineralogical Society of America, *Rev. Mineral.*, **9A**, 1-102.

Hercule, S. (1996): Cinétique et solubilité de l'hydrogène dans le diopside monocristallin. 131 p., PhD thesis, Université Paris-Sud Orsay, France.

Hercule, S. & Ingrin, J. (1999): Hydrogen in diopside: Diffusion, extraction-incorporation, and solubility. *Am. Mineral.*, **84**, 1577-1588.

Hermeling, J. & Schmalzried, H. (1984): Tracer diffusion of the Fe-cations in olivine $(Fe_xMg_{1-x})_2SiO_4$ (III). *Phys. Chem. Minerals*, **11**, 161-166.

Ihinger, P.D. & Bell, D.R. (1991): Isotropic composition of hydrogen in nominally anhydrous mantle minerals. *EOS*, **72**, 537.

Ingrin, J., Doukhan, N., Doukhan, J.C. (1992): Dislocation glide systems in diopside single crystals deformed at 800-900 °C. *Eur. J. Mineral.*, **4**, 1291-1302.

Ingrin, J. & Hercule, S. (1994): Diffusion of hydrogen in diopside and pyrope. International Mineralogical Association - 16th General Meeting Pisa. Abstracts, 183.

Ingrin, J., Hercule, S., Charton, T. (1995): Diffusion of hydrogen in diopside: Results of dehydration experiments. *J. Geophys. Res.*, **100**, 15489-15499.

Ingrin, J., Latrous, K., Doukhan, J.C., Doukhan, N. (1989): Water in diopside: an electron microscopy and infrared spectroscopy study. *Eur. J. Mineral.*, **1**, 327-341.

Inoue, T., Irifune, T., Yurimoto, H., Miyagi, I. (1998): Decomposition of K-amphibole at high pressures and implications for subduction zone volcanism. *Phys. Earth Planet. Interiors*, **107**, 221-231.

Inoue, T., Yurimoto, H., Kudoh, Y. (1995): Hydrous modified spinel, $Mg_{1.75}SiH_{0.5}O_4$: a new water reservoir in the mantle transition zone. *Geophys. Res. Lett.*, **22**, 117-120.

Irifune, T., Kubo, N., Isshiki, M., Yamasaki, Y. (1998): Phase transformations in serpentine and transportation of water into the lower mantle. *Geophys. Res. Lett.*, **25**, 203-206.

Iwamori, H. (1993): A model for disequilibrium mantle melting incorporating melt transport by porous and channel flows. *Nature*, **366**, 734-737.

Jaoul, O., Bertran-Alvarez, Y., Liebermann, R.C., Price, G.D. (1995): Fe-Mg interdiffusion in olivine up to 9 GPa at 600-900 °C; experimental data and comparison with defect calculations. *Phys. Earth Planet. Interiors*, **89**, 199-218.

Jambon, A. & Zimmermann, J.L. (1990): Water in oceanic basalts: evidence for dehydration of recycled crust. *Earth Planet. Sci. Lett.*, **101**, 323-331.

Jurewicz, A.J.G. & Watson, E.B. (1988): Cations in olivine, part 2: diffusion in olivine xenocrysts, with applications to petrology and mineral physics. *Contrib. Mineral. Petrol.*, **99**, 186-201.

Justice, M. & Graham, E. (1982): The effect of water on high-temperature deformation in olivine. *Geophys. Res. Lett.*, **9**, 1005-1008.

Karato, S. (1990): The role of hydrogen in the electrical conductivity of the upper mantle. *Nature*, **347**, 272-273.

Karato, S., Paterson, M.S., FitzGerald, J.D. (1986): Rheology of synthetic olivine aggregates: influence of grain size and water. *J. Geophys. Res.*, **91**, 8151-8176.

Kats, A., Haven, Y., Stevels, J.M. (1962): Hydroxyl groups in α–quartz. *Phys. Chem. Glasses*, **3**, 69-75.

Katsura, T. & Ito, E. (1989): The system Mg_2SiO_4-Fe_2SiO_4 at high pressure and temperatures: Precise determination of stabilities of olivine, modified spinel and spinel. *J. Geophys. Res.*, **94**, 15663-15670.

Khomenko, V.M., Langer, K., Beran, A., Koch-Müller, M., Fehr, T. (1994): Titanium substitution and OH-bearing defects in hydrothermally grown pyrope crystals. *Phys. Chem. Minerals*, **20**, 483-488.

Kitamura, M., Kondoh, S., Morimoto, N., Miller, G.H., Rossman, G.R., Putnis, A. (1987): Planar OH-bearing defects in mantle olivine. *Nature*, **328**, 143-145.

Kohlstedt, D.L., Keppler, H., Rubie, D.C. (1996): Solubility of water in the α, β and γ phases of $(Mg,Fe)_2SiO_4$. *Contrib. Mineral. Petrol.*, **123**, 345-357.

Kohlstedt, D.L. & Mackwell, S.J. (1998): Diffusion of hydrogen and intrinsic point defects in olivine. *Z. Phys. Chemie*, **207**, 147-162.

Kohn, S.C. (1996): Solubility of H_2O in nominally anhydrous mantle minerals using ^1H MAS NMR. *Am. Mineral.*, **81**, 1523-1526.

Kronenberg, A.K., Kirby, S.H., Aines, R.D., Rossman, G.R. (1986): Solubility and diffusional uptake of hydrogen in quartz at high water pressures: Implications for hydrolytic weakening. *J. Geophys. Res.*, **91**, 12723-12744.

Kronenberg, A.K., Yund, R.A., Rossman, G.R. (1996): Stationary and mobile hydrogen defects in potassium feldspar. *Geochim. Cosmochim. Acta*, **60**, 4075-4094.

Kudoh, Y., Inoue, T., Arashi, H. (1996): Structure and crystal chemistry of hydrous wadsleyite, $Mg_{1.75}SiH_{0.5}O_4$: possible hydrous magnesium silicate in the mantle transition zone. *Phys. Chem. Minerals*, **23**, 461-469.

Kurosawa, M., Yurimoto, H., Matsumoto, K., Sueno, S. (1992): Hydrogen analysis of mantle olivine by secondary ion mass spectrometry. *in* "High-pressure research: Applications to Earth and planetary sciences", Sueno, Y. & Maghnani, M., Eds., Terra Scientific, Tokyo, Japan, 283-287.

Kurosawa, M., Yurimoto, H., Sueno, S. (1997): Patterns in the hydrogen and trace element compositions of mantle olivines. *Phys. Chem. Minerals*, **24**, 385-395.

Kushiro, I. (1990): Partial melting of mantle wedge and evolution of island arc crust. *J. Geophys. Res.*, **95**, 15929-15939.

Lager, G.A., Armbruster, T., Rotella, F.J., Rossman, G.R. (1989): OH substitution in garnets: X-ray and neutron diffraction, infrared, and geometric-modelling studies. *Am. Mineral.*, **74**, 840-851.

Langer, K., Robarick, E., Sobolev, N.V., Shatsky, V.S., Wang, W. (1993): Single-crystal spectra of garnets from diamondiferous high-pressure metamorphic rocks from Kazakhstan: indications for OH^-, H_2O, and FeTi charge transfer. *Eur. J. Mineral.*, **5**, 1091-1100.

Libowitzky, E. (1999): Correlation of O-H stretching frequencies and O-H...O hydrogen bond lengths in minerals. *Mh. Chem.*, **130**, 1047-1059.

Libowitzky, E. & Beran, A. (1995): OH defects in forsterite. *Phys. Chem. Minerals*, **22**, 387-392.

Libowitzky, E. & Rossman, G.R. (1996): Principles of quantitative absorbance measurements in anisotropic crystals. *Phys. Chem. Minerals*, **23**, 319-327.

– – (1997): An IR absorption calibration for water in minerals. *Am. Mineral.*, **82**, 1111-1115.

Lu, R. & Keppler, H. (1997): Water solubility in pyrope to 100 kbar. *Contrib. Mineral. Petrol.*, **129**, 35-43.

Luth, R. & Canil, D. (1993): Ferric iron in mantle-derived pyroxenes and a new oxybarometer for the mantle. *Contrib. Mineral. Petrol.*, **113**, 236-248.

Luth, R.W., Virgo, D., Boyd, F.R., Wood, B.J. (1990): Ferric iron in mantle-derived garnets. *Contrib. Mineral. Petrol.*, **104**, 56-72.

Mackwell, S.J. (1994): Hydrogen diffusion and solubility in olivine and orthopyroxene. *Terra Abstract*, **6**, 32.

Mackwell, S.J., Dimos, D., Kohlstedt, D.L. (1988): Transient creep of olivine: Point-defect relaxation times. *Philos. Mag. A*, **57**, 779-789.

Mackwell, S.J. & Kohlstedt, D.L. (1990): Diffusion of hydrogen in olivine: Implications for water in the mantle. *J. Geophys. Res.*, **95**, 5079-5088.

Mackwell, S.J., Kohlstedt, D.L., Paterson, M.S. (1985): The role of water in the deformation of olivine single crystals. *J. Geophys. Res.*, **90**, 11319-11333.

Martin, R.F. & Donnay, G. (1972): Hydroxyl in the mantle. *Am. Mineral.*, **57**, 554-570.

McDonough, W.F. (1990): Constraints on the composition of the continental lithospheric mantle. *Earth Planet. Sci. Lett.*, **101**, 1-18.

McMillan, P.F., Akaogi, M., Sato, R., Poe, B., Foley, J. (1991): Hydroxyl groups in β-Mg_2SiO_4. *Am. Mineral.*, **76**, 354-360.

Mercier, J.C.C. (1980): Magnitude of the continental lithospheric stresses inferred from rheomorphic petrology. *J. Geophys. Res.*, **85**, 6293-6303.

Michael, P.J. (1988): The concentration behavior and storage of H_2O in the suboceanic upper mantle: implication for mantle metasomatism. *Geochim. Cosmochim. Acta*, **52**, 555-556.

Miller, G.H., Rossman, G.R., Harlow, G.E. (1987): The natural occurrence of hydroxide in olivine. *Austral. J. Chem.*, **19**, 1155-1164.

Misener, D.J. (1974): Cationic diffusion in olivine to 1400 °C and 35 kbar. *in* "Geochemical transports and kinetics", Hoffmann, A.W., Giletti, B.J., Yoder, H.S., Yund, R.A., Eds., Carnegie Institution of Washington, 117-129.

Nakamura, A. & Schmalzried, H. (1983): On the nonstoichiometry and point defects of olivine. *Phys. Chem. Minerals*, **10**, 27-37.

-- (1984): On the Fe^{2+} - Mg^{2+} inter-diffusion in olivine (II). *Ber. Bunsenges. Phys. Chem.*, **88**, 140-145.

O'Neill, H.St.C., Rubie, D.C., Canil, D., Geiger, C.A., Ross II, C.R., Seifert, F., Woodland, A.B. (1993): Ferric iron in the upper mantle and in the transition zone: Implications for relative oxygen fugacities in the mantle. *in* "Evolution of the Earth and planets". *Geophysical monographs*, 74, IUGG Vol. **14**, 73-88.

Pasteris, J.D. & Wanamaker, B.J. (1988): Laser Raman microprobe analysis of experimentally re-equilibrated fluid inclusions in olivine: Some implications for mantle fluids. *Am. Mineral.*, **73**, 1074-1088.

Paterson, M. (1982): The determination of hydroxyl by infrared absorption in quartz, silicate glasses, and similar materials. *Bull. Minéral.*, **105**, 20-29.

Patterson, J.M. & O'Connor, D.J. (1966): Chemical studies of amphibole asbestos I. Structural changes of heat-treated crocidolite, amosite and tremolite from infrared absorption studies. *Am. Mineral.*, **69**, 1116-1126.

Pawley, A.R. & Wood, B.J. (1995): The high-pressure stability of talc and 10 Å phase: Potential storage sites for H_2O in subduction zones. *Am. Mineral.*, **80**, 998-1003.

Phillips, M.W., Draheim, J.E., Popp, R.K., Clowe, C.A., Pinkerton, A.A. (1989): Effect of oxidation-dehydrogenation in tschermakitic hornblende. *Am. Mineral.*, **74**, 764-773.

Poumellec, B. & Jaoul, O. (1984): Influence of p_{O_2} and p_{H_2O} on the high temperature plasticity of olivine. *in* "Deformation of ceramics II", Tressler, R.E. & Bradt, R.C., Eds., Plenum Publ. Corp., 281-305.

Qin, Z. (1992): Disequilibrium partial melting model and its implications for trace element fractionations during mantle melting. *Earth Planet. Sci. Lett.*, **112**, 75-90.

Raterron, P., Bussod, G.Y., Doukhan, N., Doukhan, J.C. (1997): Early partial melting in the upper mantle: an A.E.M. study of a lherzolite experimentally annealed at hypersolidus conditions. *Tectonophysics*, **279**, 79-91.

Rauch, M. & Keppler, H. (1996): The solubility of water in pyroxenes. Bayerisches Forschungsinstitut für Experimentelle Geochemie und Geophysik, Annual report, 81-82.

Rossman, G.R. (1996): Studies of OH in nominally anhyrous minerals. *Phys. Chem. Minerals*, **23**, 299-304.

Rossman, G.R. & Aines, R.D. (1991): The hydrous components in garnets: Grossular-hydrogrossular. *Am. Mineral.*, **76**, 1153-1164.

Rossman, G.R., Beran, A., Langer, K. (1989): The hydrous component of pyrope from the Dora Maira Massif, Western Alps. *Eur. J. Mineral.*, **1**, 151-154.

Rossman, G.R., Rauch, F., Livi, R., Tombrello, T.A., Shi, C.R., Zhoi, Z.Y. (1988): Nuclear reaction analysis of hydrogen in almandine, pyrope and spessartite garnets. *N. Jb. Mineral. Mh.*, **1988**, 172-178.

Schmidt, M.W. (1995): Lawsonite: Upper pressure stability and formation of higher density hydrous phases. *Am. Mineral.*, **80**, 1286-1292.

Schmidt, M.W. & Poli, S. (1994): The stability of lawsonite and zoisite at high pressures: Experiments in CASH to 92 kbar and implications for the presence of hydrous phases in subducted lithosphere. *Earth Planet. Sci. Lett.*, **124**, 105-118.

Schreyer, W. (1988): Experimental studies on metamorphism of crustal rocks under mantle pressures. *Mineral. Mag.*, **52**, 1-26.

Schwandt, C.S., Cygan, R.T., Westrich, H.R. (1995): Mg self-diffusion in pyrope garnet. *Am. Mineral.*, **80**, 483-490.

Sisson, T.W. & Layne, G.D. (1993): H_2O in basalt and basaltic andesite glass inclusions from four subduc-

tion-related volcanoes. *Earth Planet. Sci. Lett.*, **117**, 619-635.

Skogby, H. (1994): OH incorporation in synthetic clinopyroxene. *Am. Mineral.*, **79**, 240-249.

Skogby, H., Bell, D.R., Rossman, G.R. (1990): Hydroxide in pyroxene: Variations in the natural environment. *Am. Mineral.*, **75**, 764-774.

Skogby, H. & Rossman, G.R. (1989): OH^- in pyroxene: An experimental study of incorporation mechanism and stability. *Am. Mineral.*, **74**, 1059-1069.

-- (1991): The intensity of amphibole OH bands in the infrared absorption spectrum. *Phys. Chem. Minerals*, **18**, 64-68.

Smyth, J.R. (1987): β-Mg_2SiO_4: A potential host for water in the mantle. *Am. Mineral.*, **72**, 1051-1055.

- (1988): Electrostatic characterization of oxygen sites in minerals. *Geochim. Cosmochim. Acta*, **53**, 1101-1110.

- (1994): A crystallographic model for hydrous wadsleyite (β-Mg_2SiO_4): An ocean in the earth's interior? *Am. Mineral.*, **79**, 1021-1024.

Smyth, J.R., Bell, D.R., Rossman, G.R. (1991): Incorporation of hydroxyl in upper-mantle clinopyroxenes. *Nature*, **351**, 732-735.

Sobolev, A.V. & Chaussidon, M. (1996): H_2O concentrations in primary melts from supra-subduction zones and mid-ocean ridges: Implications for H_2O storage and recycling in the mantle. *Earth Planet. Sci. Lett.*, **137**, 45-55.

Stixrude, L. (1997); Structure and sharpness of phase transitions and mantle discontinuities. *J. Geophys. Res.*, **102**, 14835-14852.

Sykes, D., Rossman, G.R., Veblen, D.R., Grew, E.S. (1994): Enhanced H and F incorporation in borian olivine. *Am. Mineral.*, **79**, 904-908.

Thompson, A.B. (1992): Water in the Earth's upper mantle. *Nature*, **358**, 295-302.

Ulmer, P. & Trommsdorff, V. (1995): Serpentine stability to mantle depths and subduction-related magmatism. *Science*, **268**, 858-861.

Wang, L., Zhang, Y., Essene, E. (1996): Diffusion of the hydrous component in pyrope. *Am. Mineral.*, **81**, 706-718.

Wilkins, R.W. & Sabine, W. (1973): Water content of some nominally anhydrous silicates. *Am. Mineral.*, **58**, 508-516.

Withers, A.C., Wood, B.J., Carroll, M.R. (1998): The OH content of pyrope at high pressure. *Chemical Geol.*, **147**, 161-171.

Wood, B.J. (1995): The effect of H_2O on the 410-km seismic discontinuity. *Science*, **268**, 74-76.

Wright, K. & Catlow, C.R.A. (1994): A computer simulation study of (OH) defects in olivine. *Phys. Chem. Minerals*, **20**, 515-518.

Wright, K., Freer, R., Catlow, C.R.A. (1994): The energetics and structure of the hydrogarnet defect in grossular: a computer simulation study. *Phys. Chem. Minerals*, **20**, 500-503.

Wyllie, P.J. (1979): Magmas and volatile components. *Am. Mineral.*, **64**, 469-500.

Young, T.E., Green II, H.W., Hofmeister, A.M., Walker, D. (1993): Infrared spectroscopic investigation of hydroxyl in β-$(Mg,Fe)_2SiO_4$ and coexisting olivine: Implications for mantle evolution and dynamics. *Phys. Chem. Minerals*, **19**, 409-422.

Yusa, H. & Inoue, T. (1997): Compressibility of hydrous wadsleyite (β-phase) in Mg_2SiO_4 by high pressure X-ray diffraction. *Geophys. Res. Lett.*, **24**, 1831-1834.

Received 1 April 1999
Modified version received 30 November 1999
Accepted 20 January 2000